HYPERFINE AND ELECTRIC QUADRUPOLAR INTERACTION-DRIVEN LOSCHMIDT ECHO IN NANOSCALE NUCLEAR SPIN BATHS

A THESIS SUBMITTED TO

THE GRADUATE SCHOOL OF ENGINEERING AND SCIENCE

OF BILKENT UNIVERSITY

IN PARTIAL FULFILLMENT OF THE REQUIREMENTS FOR

THE DEGREE OF

MASTER OF SCIENCE

IN

PHYSICS

By

Ekrem Taha Güldeste

July 2018

HYPERFINE AND ELECTRIC QUADRUPOLAR INTERACTION-DRIVEN LOSCHMIDT ECHO IN NANOSCALE NUCLEAR SPIN BATHS

By Ekrem Taha Güldeste

July 2018

We certify that we have read this thesis and that in our opinion it is fully adequate, in scope and in quality, as a thesis for the degree of Master of Science.

Ceyhun Bulutay(Advisor)

Mehmet Cemal Yalabık

Sadi Turgut

Approved for the Graduate School of Engineering and Science:

Ezhan Karaşan
Director of the Graduate School

ABSTRACT

HYPERFINE AND ELECTRIC QUADRUPOLAR INTERACTION-DRIVEN LOSCHMIDT ECHO IN NANOSCALE NUCLEAR SPIN BATHS

Ekrem Taha Güldeste
M.S. in Physics
Advisor: Ceyhun Bulutay
July 2018

Environmental dynamics in solid state matrix is of much importance for quantum information processing and storage purposes. Here, we first give a basic recipe to get Loschmidt echo (LE) which is a measure of decoherence (loss of information from the qubit) in heterogeneously interacting nuclear spin bath (NSB) in the presence of Fermi-contact hyperfine and nuclear spin dipole-dipole interactions. Then, by dropping the latter we discuss the basic dependencies of pure-dephasing regime on size, initial polarization, hyperfine coupling inhomogeneity, spin quantum number in nuclear spin environments, and arrive at a phenomenological expression that governs all these attributes. For NSBs consisting of spin-$I \geq 1$, the effect of nuclear electric quadrupole interaction is also considered where its biaxiality term has an influence on the decoherence process. Furthermore, a general decoherence channel is also employed to see how phase-flip rate affects LE. After insights gained from these models, we consider two generic realistic systems, namely, donor center and quantum dot and explain the power spectral density of LE in these cases.

Keywords: qubit decoherence, central spin decoherence, Loschmidt echo, nuclear spin baths.

ÖZET

NANO ÖLÇEKLİ SPİN HAMAMLARI İÇİN ENALTYAPI VE DÖRTKUTUP ETKİLEŞİMLERİ ALTINDA LOSCHMIDT YANKISI

Ekrem Taha Güldeste
Fizik, Yüksek Lisans
Tez Danışmanı: Ceyhun Bulutay
Temmuz 2018

Katı hal matrisinde çevresel dinamikler kuantum bilgi işleme ve depolama amaçları için çok önemlidir. Burada, öncelikle Fermi-temas enaltyapı ve nükleer çiftkutup etkileşiminin varlığında, nükleer spin hamamının eşevresizliğini ölçmek için Loschmidt yankısını (LE) elde ettiğimiz temel bir reçete verilmektedir. Daha sonra, sadece enaltyapı etkileşinin varlığında, saf faz bozunumu rejiminin, hamam büyüklüğü, kutuplu hamam, enaltyapı etkileşiminin sapması, hamamdaki spin kuantum özdeğeri gibi özelliklerin Loschmidt yankısına etkisini inceleyip, bu değişken uzayında geçerli olan olgusal bir ifadeyi sunmaktayız. Bununla beraber, dörtkutup etkileşiminin etkili olduğu, Spin-$I \geq 1$ şartını sağlayan spin hamamlarının faz bozunumu sürecinide ele almaktayız. Safsızlık merkezi ve kuantum nokta modellemelerini kapsayan gerçekçi modellere geçmeden önce ise faz-dönmeli kanalın spin eşevresiliğine etkisi incelemekteyiz.

Anahtar sözcükler: kuantum-bit eşevresizliği, merkez spin eşevresizliği, Loschmidt yankısı, nükleer spin hamamı.

Acknowledgement

First of all, I would like to express my sincere gratitude to my advisor Prof. Dr. Ceyhun Bulutay for the continuous support, patience, guidance, motivation, and immense knowledge over the last seven years. I could not have imagined having a better advisor and mentor during my undergraduate and graduate study. Without him academic life would be insufferably hard.

Besides my advisor, I would like to thank the rest of my thesis committee: Prof. Dr. M. Cemal Yalabık and Prof. Dr. Sadi Turgut for their encouragement, insightful comments and questions, but also for sparing their valuable times.

This thesis is an outgrowth of the TÜBİTAK under Project No:114F409, through which my fellowship has been granted in the last three years.

I acknowledge my colleague, Mustafa Kahraman, for many valuable discussions and more importantly, for his friendship. It has been a pleasure for me to have a chance to work with him in the same group.

I would like to thank to my other groupmate, Yağmur Aksu Korkmaz, for contributions to the various domains and friendship.

I present my specially thanks to Burak Kakillioğlu and Ömer Faruk Karadavut for nice video chats and their warm friendship during past years.

I send lots of love to Fatih Altındiş and Selim Han Türer for their valuable friendship and conversations along those hard research days.

I am thankful to my high school friends, Hasan Özkara, Mustafa Kılıçarslan, Yahya Ünalan, Samet Çelik, Murat Keskin, Mahmut Ayvazoğlu and Emir Yasin Kekeç, who preserve their special positions.

I am indebted to my parents, Hatice and Ayhan, my grandmother, Müşerref, my sister, İkbal Vildan, my brother, Mustafa Talha, and his wife, Göknur, for

their great understanding and support during my studies. This thesis would not have been possible without their support. I deeply appreciate them for encouraging me to follow my dreams and their belief in me.

This work is dedicated to my fiancée, Hilal, with my deepest gratitude and love, for her patient, understanding, encouragement and constant emotional support.

Contents

List of Figures

Chapter 1

Introduction

Nuclear spins that are in a semiconductor environment are electrically isolated from charge noise, this endowes them long coherence lifetimes exceeding a second at room temperatures unlike the electron spins which decohere a few orders faster due to environmental fluctuations [1]. Charge immunity of nuclear spins makes them good candidates to be used for various quantum information processing (QIP) tasks such as quantum registers and gate operation processes [2, 3, 4, 5, 6]. For most of these cases, possible electrical [7] and optical [8] manipulation methods have been addressed in quantum dot or defect center environments where an intermediary electron spin used as the qubit. For the spin systems that consist of both electron and nuclear spins, the hyperfine (hf) is the primary interaction that governs the decoherence process [9, 10, 11, 12].

Foremost, this topic is related to so-called central spin model (CSM) which has been studied to describe the decoherence of electron spin by different groups [13, 14, 15, 16], but even so, it will be very useful to approach this model from nuclear spin bath (NSB) perspective. One of the main enthusiasm associated with the hf-driven NSBs comes from two electron qubit entanglement via reservoir [17]. Most notably, this is possible without any restriction on initial NSB state other than letting NSB to interact two qubits alternatingly. Or, polarized NSB can be employed as a quantum interface for optical fields to achieve high fidelity levels

of quantum information for input and output field [18].

The need for a comprehensive understanding of the hyperfine interaction (HFI)-driven NSB is triggered by these facts and can be exploited by the Loschmidt echo (LE) which is interpreted as a return probability of a bath to its initial state [19]. Therefore, the flow of the quantum information from the two-level system (namely a spin qubit) through the bifurcated environment (NSB) can be probed, thanks to LE [20] which is also experimentally accessible via nuclear magnetic resonance tools [21, 22].

1.1 What is this thesis about?

At this stage, the physical relevance of the model must be clearly stated for the thesis to be put into a perspective. For the most part, we shall be dealing with Fermi-contact HFI in this work which is effective on the conduction band electrons in semiconductors. For both second and third chapter we included secular part in which the longitudinal part of HFI does not take place, since, it is possible to detune this part in data storage process [23, 24]. The *indirect* HFI can be ignored if the Knight field due to electron is high enough [25] which leads extra nuclear spin precession process [26, 27, 28]. Furthermore, Zeeman splitting of nuclear spins can be omitted due to weak nuclear magnetic moments [29] when compared to the HFI.

Second Chapter discusses the HFI alongside with intrabath nuclear dipole-dipole (dd) interaction which is exactly solvable model by means of Jordan-Wigner transformation. It is noteworthy that this method is straightforward when dd interaction within the bath is uniform, yet, for the non-uniform coupling regime it becomes useful method as a mathematical warm up. Moreover, it provides an idea for the most basic characteristics of LE and forces us to exploit the third chapter which is the most essential part of this thesis.

When short time scales is of a concern, the dd coupling regime can be ignored as

discussed in the introduction section of third chapter in detail. This simplification gives the opportunity to study NSBs from much wider perspective. Importantly, we discuss NSBs under pure dephasing model and separately analyse various key parameter for both temporal and spectral behaviours of LE. Quadrupolar Interaction (QI) is also considered in addition to HFI, to construct two realistic models: Donor impurity and Quantum Dot. Additionally, the effect of a phase-flip channel to LE is also discussed as a generic decoherence source.

The appendix consists of step by step derivations in detail relevant to Jordan-Wigner transformation of chapter two to fill some sizable gaps in between equations.

Chapter 2

Interacting spin chain: exactly solvable many-body systems

2.1 Model Hamiltonian

This chapter discusses homogeneous and inhomogeneous 1D-XY spin-1/2 chains which are coupled to the central spin (CS) to observe how it decoheres with time. It serves to exemplify an exactly solvable many-body technique under the name Jordan-Wigner transformation. The basic algorithm is to map chain spins into spinless fermionic particles, take the Fourier transform to diagonalize Hamiltonian and then, connect two ground states by writing them in BCS-like form and calculate the Loschmidt echo for decoherence. This is schematically shown on the flow-chart. The model Hamiltonian of the spin chain of N nuclear spins is of the form,

$$H = -\sum_{i=1}^{N} J_{i,i+1}\Big[\frac{1+\gamma}{2}\sigma_i^x\sigma_{i+1}^x + \frac{1-\gamma}{2}\sigma_i^y\sigma_{i+1}^y\Big] - \sum_{i=1}^{N}\lambda_i\sigma_i^z, \tag{2.1}$$

where i is the site index, J is coupling constant between nearest neighbor spins, γ is anisotropy factor in xy plane, σ^α are Pauli spin operators ($\alpha = (x, y, z)$) and λ_i is the hyperfine interaction constant between CS and chain spins.

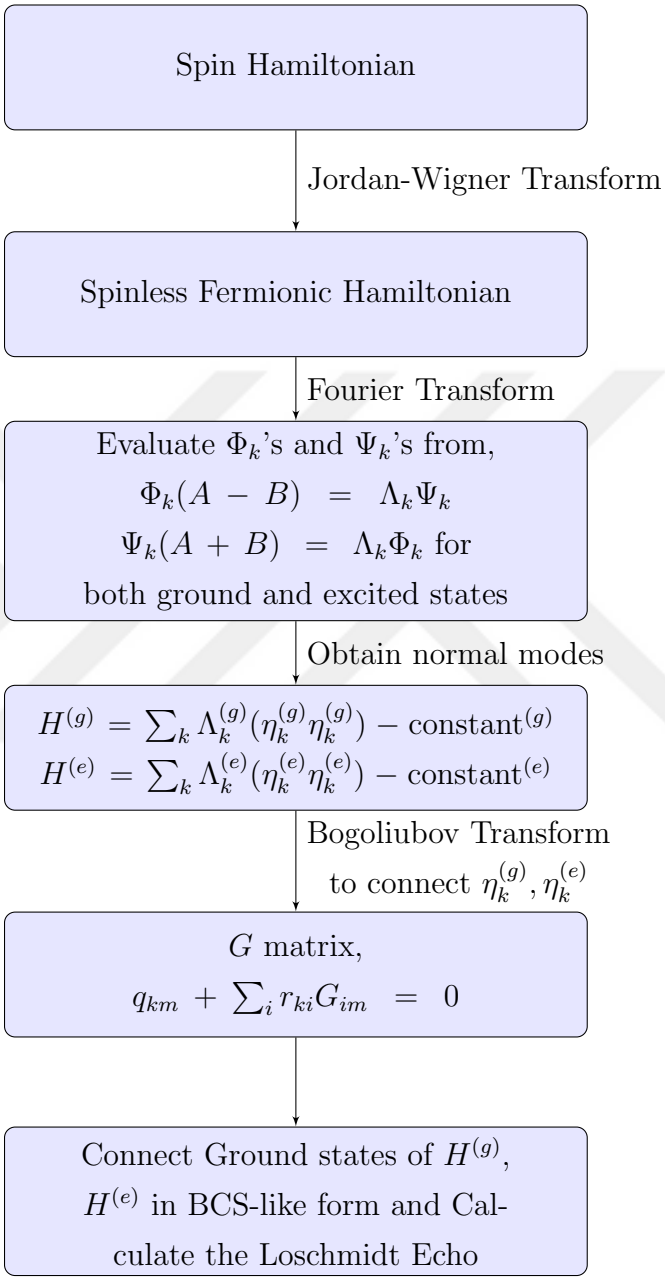

2.2 Diagonalization of homogeneous spin chain

For a homogeneous spin chain all coupling constants between neighbors are taken as equal and set to 1. Also, for the sake of simplicity we assume that hyperfine interaction constants are also the same (i.e. $J_{i,i+1} = J = 1$ and $\lambda_i = \lambda$). Then

Eq. (2.1) reduces to,

$$H = -\sum_{i=1}^{N} \Big[\frac{1+\gamma}{2}\sigma_i^x\sigma_{i+1}^x + \frac{1-\gamma}{2}\sigma_i^y\sigma_{i+1}^y - \lambda\sigma_i^z\Big], \tag{2.2}$$

It is possible to write Eq. (2.2) in terms of raising and lowering operators which are given by,

$$\sigma^+ = (\sigma^x + i\sigma^y)/2, \tag{2.3}$$

$$\sigma^- = (\sigma^x - i\sigma^y)/2. \tag{2.4}$$

Substituting to Eq. (2.2) yields,

$$H = -\sum_{i=1}^{N}[\sigma_i^+\sigma_{i+1}^- + \sigma_i^-\sigma_{i+1}^+ + \gamma(\sigma_i^+\sigma_{i+1}^+ + \sigma_i^-\sigma_{i+1}^-) - \lambda\sigma_i^z]. \tag{2.5}$$

Observe that setting $\gamma = 0$ leaves us with only spin flip-flop term, and for any non-zero γ, flip-flip and flop-flop interactions are also allowed.

2.3 Jordan-Wigner transformation

It is straightforward to diagonalize Hamiltonian in (2.5) by means of Jordan-Wigner Transformation. Noting that for an SU(2) group, $(\sigma_i^+)^2 = (\sigma_i^-)^2 = 0$, one can easily establish a connection between spin operators and spinless fermionic operators, where the similar conditions are satisfied [30],

$$c_i^{\dagger^2} = c_i^2 = 0, \tag{2.6}$$

$$[c_i^\dagger, c_j]_+ = \delta_{ij}, \tag{2.7}$$

where $c^\dagger$ and c are fermionic creation and annihilation operators, respectively. These relations allow us to make following mapping,

$$c^\dagger|0\rangle = |\uparrow\rangle, \tag{2.8}$$

$$|0\rangle = |\downarrow\rangle, \tag{2.9}$$

where $|0\rangle$ is the vacuum state. Establishing fermionic number operator $n_i = c_i^\dagger c_i$ enables us to distinguish between $|\uparrow\rangle$ and $|\downarrow\rangle$ states just by giving one site fermionic state or empty site. That is, if we represent $|\uparrow_i\rangle$ state by $|f_i\rangle$ then we have,

$$n_i|f_i\rangle = |f_i\rangle, \tag{2.10}$$

$$n_i|0\rangle = 0. \tag{2.11}$$

Now, we are ready to define spin operators in terms of fermionic creation and annihilation operators,

$$\sigma_i^- = e^{\left(i\pi \sum_{j=1}^{i-1} c_j^\dagger c_j\right)} c_i, \tag{2.12}$$

$$\sigma_i^+ = c_i^\dagger e^{\left(-i\pi \sum_{j=1}^{i-1} c_j^\dagger c_j\right)}, \tag{2.13}$$

$$\sigma_i^z = 2c_i^\dagger c_i - 1, \tag{2.14}$$

where the exponentials are just a phase factor to ensure that commutation relations of different spin sites are satisfied. Let's calculate,

$$e^{i\pi c_i^\dagger c_i} = \sum_{n=0}^{\infty} \frac{(i\pi)^n}{n!} (c_i^\dagger c_i)^n = 1 + \Big(\sum_{n=}^{\infty} \frac{(i\pi)^n}{n!} \Big) c_i^\dagger c_i = 1 + (e^{i\pi} - 1) c_i^\dagger c_i = 1 - 2c_i^\dagger c_i. \tag{2.15}$$

Here, we have used to fact that $(c_i^\dagger c_i)^n = c_i^\dagger c_i$ for all non-zero integer n. Then the total phase factor can be expressed as,

$$P_i = \prod_{j=1}^{i-1} (1 - 2c_j^\dagger c_j). \tag{2.16}$$

Then, terms in Eq. (2.5) can be written as follows,

$$\begin{aligned}
\sigma_i^+\sigma_{i+1}^- &= c_i^\dagger[P_jP_{j+1}]c_{i+1} \\
&= c_i^\dagger[\prod_{j=1}^{i-1}(1-2c_j^\dagger c_j)^2(1-2c_i^\dagger c_i)]c_{i+1} \\
&= c_i^\dagger[\prod_{j=1}^{i-1}(1-4c_j^\dagger c_j+4(c_j^\dagger c_j)^2)(1-2c_i^\dagger c_i)]c_{i+1} \\
&= c_i^\dagger[\prod_{j=1}^{i-1}(1-4c_j^\dagger c_j+4c_j^\dagger c_j)(1-2c_i^\dagger c_i)]c_{i+1} \\
&= c_i^\dagger(1-2c_i^\dagger c_i)c_{i+1} \\
&= (c_i^\dagger-2c_i^{\dagger^2}c_i)c_{i+1} \\
&= c_i^\dagger c_{i+1}. \qquad (2.17)
\end{aligned}$$

Similarly, other terms can be written as,

$$\sigma_i^-\sigma_{i+1}^+ = -c_ic_{i+1}^\dagger, \qquad (2.18)$$

$$\sigma_i^+\sigma_{i+1}^+ = c_i^\dagger c_{i+1}^\dagger, \qquad (2.19)$$

$$\sigma_i^-\sigma_{i+1}^- = -c_ic_{i+1}. \qquad (2.20)$$

So that Hamiltonian in Eq. (2.5) takes the form [31],

$$H = -\sum_{i=1}^{N}\left[(c_i^\dagger c_{i+1}+c_{i+1}^\dagger c_i)+\gamma[c_i^\dagger c_{i+1}^\dagger+c_{i+1}c_i]-2\lambda[c_i^\dagger c_i-1/2]\right], \qquad (2.21)$$

which can also be written in a more compact form[1] [31],

$$H = \sum_{i,j}^{N} c_i^\dagger A_{ij}c_j+\frac{1}{2}(c_i^\dagger B_{ij}c_j^\dagger+c_jB_{ji}c_i), \qquad (2.22)$$

where,

$$A = -\begin{pmatrix} 2\lambda & 1 & & & 1 \\ 1 & 2\lambda & 1 & \mathbf{0} & \\ & 1 & 2\lambda & 1 & \\ & \mathbf{0} & 1 & & \\ 1 & & & & \ddots \end{pmatrix}, \qquad (2.23)$$

[1]We have used periodic boundary conditions (PBC).

and,

$$B = \gamma \begin{pmatrix} 0 & -1 & & & 1 \\ 1 & 0 & -1 & \mathbf{0} & \\ & 1 & 0 & -1 & \\ & \mathbf{0} & 1 & & \\ -1 & & & & \ddots \end{pmatrix}. \tag{2.24}$$

Here note that in Eq. (2.22), $\frac{1}{2}$ factor has appeared as coefficient to prevent us from double counting. The goal is to put this Hamiltonian into the form,

$$H = \sum_{k=1}^{N} \Lambda_k \eta_k^\dagger \eta_k + \text{constant} \tag{2.25}$$

Looking for canonical operators of the form [32],

$$\eta_k^\dagger = \sum_{i=1}^{N} g_{ki} c_i^\dagger + h_{ki} c_i, \tag{2.26}$$

$$\eta_k = \sum_{i=1}^{N} g_{ki} c_i + h_{ki} c_i^\dagger. \tag{2.27}$$

Let,

$$\Phi_{kj} = g_{kj} + h_{kj}, \tag{2.28}$$

$$\Psi_{kj} = g_{kj} - h_{kj}. \tag{2.29}$$

Then, one can find g_{kj} and h_{kj} such that (See Appendix $A.1$ for detailed derivation),

$$\Phi_k(A - B) = \Lambda_k \Psi_k, \tag{2.30}$$

$$\Psi_k(A + B) = \Lambda_k \Phi_k, \tag{2.31}$$

which are obviously coupled equations. One can choose row vectors Φ_k ,Ψ_k to be orthonormal[2] and also it is allowed take positive Λ_k values. Now it is possible to decouple (2.30) and (2.31) as[3],

$$\Phi_k(A - B)(A + B) = \Lambda_k^2 \Phi_k. \tag{2.32}$$

[2]The orthonormality of Φ_k, makes Ψ_k normalized directly.

[3]Here we write the equation for vector (Φ_k) only since the other decoupled equation will not be necessary.

Once Φ_k are determined, Ψ_k can be found from (2.31). Under the constraint that $\eta_k^\dagger$, η_k need to be canonical it is straightforward to deduce constraints [4] (See $A.2$),

$$\sum_i (g_{ki}h_{ni} + h_{ki}g_{ni}) = 0. \tag{2.33}$$

$$\sum_i (g_{ki}g_{ni} + h_{ki}h_{ni}) = \delta_{ij}, \tag{2.34}$$

2.4 Loschmidt echo

Assuming that the CS is in a pure state at $t = 0$, the whole wave function can be expressed as a direct product of CS and a bath state [34],

$$|\Psi(0)\rangle = (c_g|g\rangle + c_e|e\rangle) \otimes |B(0)\rangle, \tag{2.35}$$

and after a time evolution at time t it becomes,

$$|\Psi(t)\rangle = c_g|g\rangle \otimes |B(t)^{(g)}\rangle + c_e|e\rangle \otimes |B(t)^{(e)}\rangle. \tag{2.36}$$

Suppose we have two different Hamiltonians which are already diagonalized by JW transformation with the following forms,

$$H^{(g)} = \sum_k \Lambda_k^{(g)}(\eta_k^{(g)}\eta_k^{(g)}) - \text{constant}^{(g)}, \tag{2.37}$$

$$H^{(e)} = \sum_k \Lambda_k^{(e)}(\eta_k^{(e)}\eta_k^{(e)}) - \text{constant}^{(e)}, \tag{2.38}$$

so that,

$$\begin{pmatrix} \eta^{(g,e)} \\ \eta^{(g,e)\dagger} \end{pmatrix} = U^{(g,e)} \begin{pmatrix} c \\ c^\dagger \end{pmatrix}. \tag{2.39}$$

where $U^{(g,e)}$ are both unitary matrices. Then it is possible to connect operators of ground and excited states by,

$$\begin{pmatrix} \eta^{(g)} \\ \eta^{\dagger(g)} \end{pmatrix} = U^{(g)}U^{(e)-1} \begin{pmatrix} \eta^{(e)} \\ \eta^{\dagger(e)} \end{pmatrix}, \tag{2.40}$$

[4] There is a sign mistake in Ref. [32] and [33] for the Eq. (2.33).

where,

$$U^{(g,e)} = \begin{pmatrix} g^{(g,e)} & h^{(g,e)} \\ h^{*(g,e)} & g^{*(g,e)} \end{pmatrix}. \tag{2.41}$$

Here one can find $h^{*(g,e)}$, $g^{*(g,e)}$ from linear combinations of $\Phi^{*(g,e)}$, $\Psi^{*(g,e)}$. Loschmidt Echo (LE) is the overlap of a state which evolves with two different Hamiltonian,

$$M(t) = |\langle B^{(g)}(t)|B^{(e)}(t)\rangle|^2, \tag{2.42}$$

obviously $B^{(g)}(t)$ is bath state and $\langle B^{(g)}(0)|B^{(e)}(0)\rangle = 1$. Here, we assume that $B^{(g)}$ is the ground state of Hamiltonian $H^{(g)}$. It is possible to connect to states $B^{(g)}$ and $B^{(e)}$ in BCS-like form [35],

$$|B^{(g)}\rangle = \frac{1}{\Upsilon} e^{1/2 \sum_{i,j} \eta_i^{(e)\dagger} G_{ij} \eta_j^{(e)\dagger}} |B^{(e)}\rangle, \tag{2.43}$$

where Υ is some normalization constant and elements of G can be found from $q_{km} + \sum_i r_{ki} G_{im} = 0$. which is derived in Appendix $A.3$ [5]. Then, one can find LE as,

$$|\langle B^{(g)}(t)|B^{(e)}(t)\rangle|^2 = \frac{1}{\Upsilon^4} \prod_{i,j>i} \Big[(1+|G_{ij}|^2)^2 - 4(1+|G_{ij}|^2)^2 \sin^2\Big(\frac{\Lambda_i^{(e)} + \Lambda_j^{(e)}}{2} t\Big)\Big]. \tag{2.44}$$

To show the power of this exact framework, we should mention that the numerical exact diagonalization obtained from master equation solves are amenable only for small spin chains ($N < 21$) due to exponential growth of Hilbert space. Whereas, Jordan-Wigner diagonalization is much more CPU friendly, since implementing (2.44) requires only 3 nested `for` loops. Fig. 2.4 shows the qubit coherence for site dependent coupling constants J_i. Notice that the expression (2.44) is only valid for ground state of $H^{(g)}$, initial state $|B(0)\rangle$, for exact diagonalization method must be seeded accordingly[6].

Loschmidt Echo can be interpreted as a measure of entanglement; while $M = 1$ qubit is completely disentangled from the bath, $M = 0$ represents entangled state, meaning loss of information to the reservoir. Figs. 2.2-2.4 show LE for different

[5] We are doubtful about the correctness of Eq. (B7) in ref. [35].

[6] Fig. 2 of Ref. [36] has been reproduced. in fig 2.2

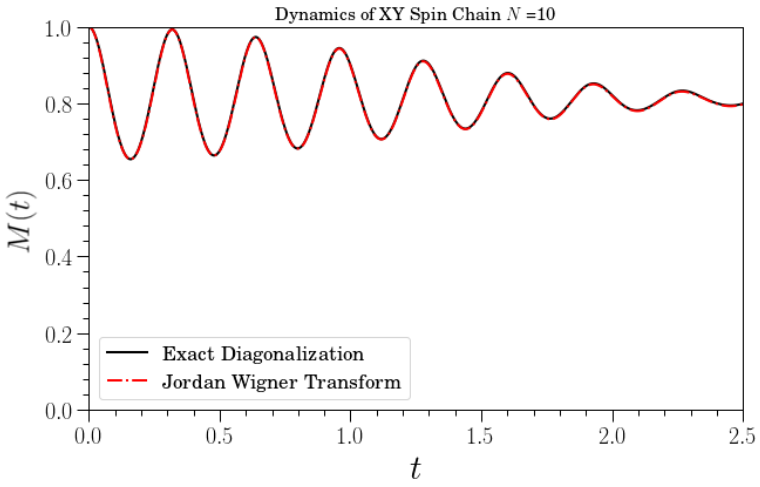

Figure 2.1: Loschmidt echo as a function of time. $N = 10$, $\gamma = 1.0$, $\lambda^{(g)} = 1.0$, $\lambda^{(e)} = 5.0$, $J = [0, 1]$. Comparison of Exact Diagonalization (numerical) vs JW transformation method. Difference between two curves is not distinguishable.

parameter sets, note that at $t = 0$ all plots start from $M = 1$, meaning qubit and NSB starts completely disentangled initially. In fig 2.4 we normalize time scale with respect to mean value of HFI coupling constant to observe when the dd coupling dominates the system. In realistic cases dd interaction is three orders of magnitude smaller than the HFI, and can be practically omitted for short time scales since dd coupling shows its presence if the condition, $\bar{J}/\bar{\lambda}^{(e)} \geq 0.1$, is satisfied.

In the remainder of this thesis, we shall not be using the JW technique as we found the one-body hyperfine and quadrupolar interactions to be much more important on LE for the temporal scale that we are interested in.

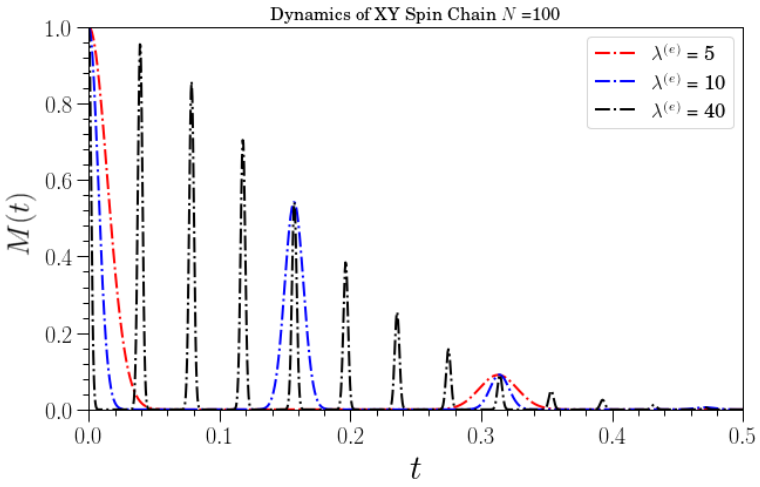

Figure 2.2: Loschmidt echo for different $\lambda^{(e)}$ values. $N = 100$, $\gamma = 1.0$, $\lambda^{(g)} = 0$, $J = 1$.

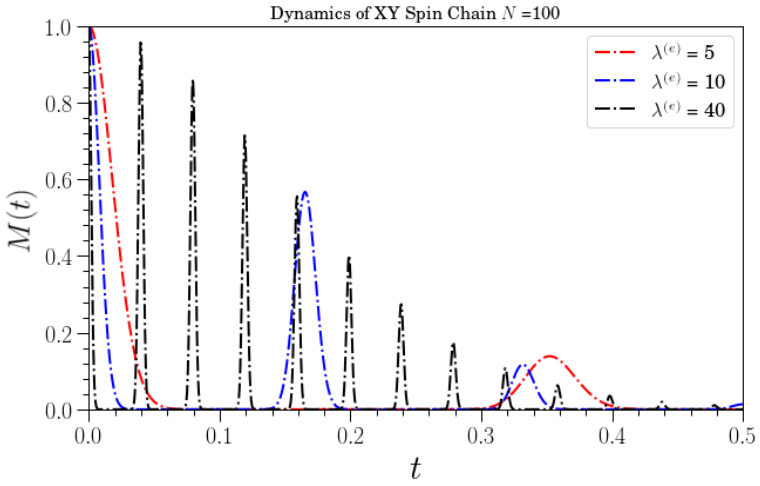

Figure 2.3: Loschmidt echo for different $\lambda^{(e)}$ values. $N = 100$, $\gamma = 1.0$, $\lambda^{(g)} = 1.0$, $J = 1$.

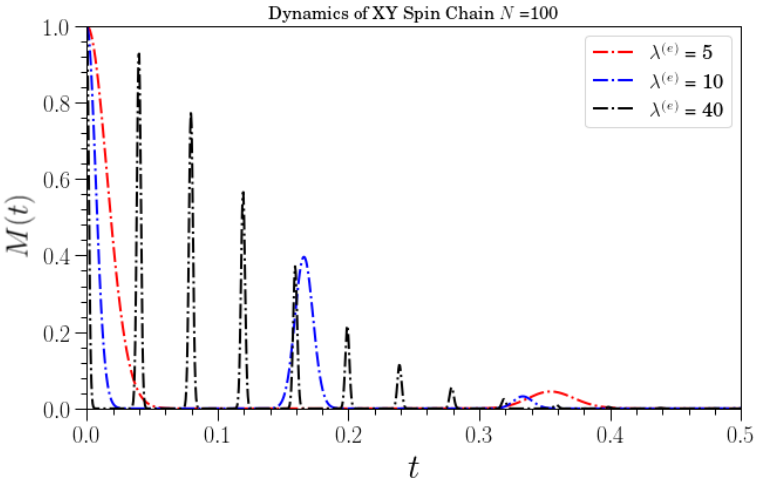

Figure 2.4: Loschmidt echo for different $\lambda^{(e)}$ values. $N = 100$, $\gamma = 1.0$, $\lambda^{(g)} = 1.0$, $J = [0, 2]$.

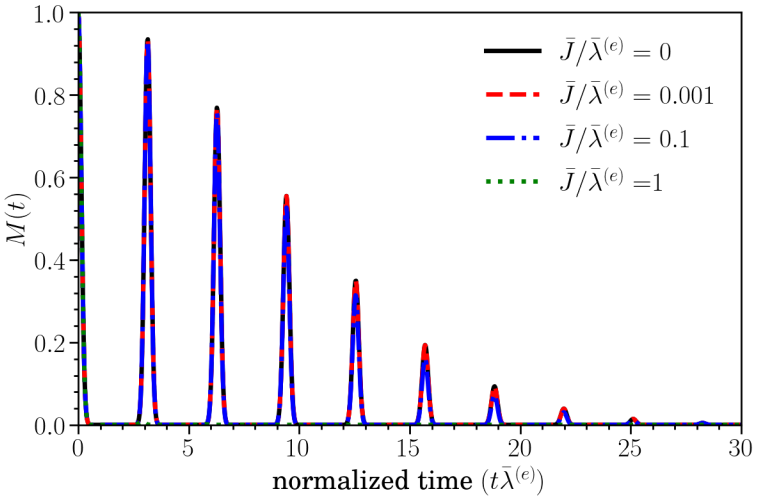

Figure 2.5: Loschmidt echo for various dd coupling strengths values as. Here time scale is normalized by $\bar{\lambda}^{(e)} = \sum_{i=1}^{N} \lambda_i$. $N = 50$, $\gamma = 1.0$, $\lambda^{(g)} = 0$, $J = [0, 2]$.

Chapter 3

Short-time dynamics of Loschmidt echo in nano-scale nuclear spin baths

Even though, JW-diagonalization can provide an exact expression for LE, it is restricted to the ground state of spin-1/2 spin chain. Furthermore, it is limited to spin-1/2 NSB which has been extensively studied [2, 3, 4, 5, 6, 8, 15, 17, 18, 37] in the literature, despite the fact that group III-V semiconductors consist of $I \geq 1$ nuclei [29] in which quadrupolar interaction (QI) should be considered. All of these brings us to main subject of this chapter where we flourish the basic characteristics of 1-body interactions, HFI and QI namely, to develop profound understanding NSB's temporal and spectral dynamics of LE by investigating bath size, coupling nonuniformity, polarization of initial state, and the nuclear spin quantum number, I dependencies of the NSB.[1]

One may have some worries about sacrifacing dd interaction that have been considered in previous chapter, yet because of the static lattice spacing in solid state matrix which restricts closeness of two neighboring nuclear spins, this makes it smaller more than three orders of magnitude in frequency when compared to

[1] Contents of this chapter are reported in Ref. [38].

the HFI, so that, dd interaction corresponds to miliseconds in time scale and can be ignored especially if short time scales is of a concern [6, 9, 10].

3.1 Basic formalism for hyperfine interaction mediated Loschmidt echo

When terms associated with the dd interaction in Eq. (2.1) are dropped out, Hamiltonian remains with secular part of HFI, so-called pure dephasing model. Spin qubit with *non*-interacting spin chain allows us to employ analytic expression for LE in straightforward manner, providing various degree of freedoms upon the choice of NSBs at the same time which are going to be discussed in detail in following sections.

3.1.1 Hyperfine interaction with the central spin

The spin qubit consist of two level basis ($|\uparrow\rangle$, $|\downarrow\rangle$) interacting with nuclear spin-I environment which forms the bath sector via transverse part of HFI. In the scope of this chapter, homospin-I environment, where the I value changes from 1/2 to 9/2, is choosen for simplicity even our model allows heterogeneous NSBs. As mentioned, thanks to interested time scale for HFI interaction, qubit and NSB together can be considered as a closed system (the open system approximations can also be made see Sec. 3.1.4). Now it is possible to define pure dephasing Hamiltonian as [39],

$$\hat{H} = \hat{H}_+ \otimes |\uparrow\rangle\langle\uparrow| + \hat{H}_- \otimes |\downarrow\rangle\langle\downarrow| \,, \tag{3.1}$$

where each nuclear spin is conditioned on the two level basis as: $|\uparrow\rangle \rightarrow \hat{H}_+$, $|\downarrow\rangle \rightarrow \hat{H}_-$, with

$$\hat{H}_\pm = \pm \sum_i A_i \hat{I}_i^z \,, \tag{3.2}$$

where $\hat{I}_i^z$ is the zth component of i'th nuclear spin operator along the quantization axis of the qubit, and A_i is the hf coupling strength in frequency.

3.1.2 Loschmidt echo

It is possible to probe quantum coherence via, creating central spin state as a linear combination of spin up and down states (*i.e.* $|\psi\rangle = C_+ |\uparrow\rangle + C_- |\downarrow\rangle$) which is set to be completely uncorrelated with its environment $|B_0\rangle$ at $t = 0$, so that overall system can be expressed with the tensor product of the two,

$$|\Psi(t=0)\rangle = |\psi\rangle \otimes |B_0\rangle \ . \tag{3.3}$$

For some arbitrary time t, system propagates under the Hamiltonian given in Eq. (3.1) resulting into some entangled state,

$$|\Psi(t)\rangle = C_+ |\uparrow\rangle \otimes |B_+(t)\rangle + C_- |\downarrow\rangle \otimes |B_-(t)\rangle \ . \tag{3.4}$$

Central spin and NSB's entanglement indicates qubit decoherence which can be tracked down by LE, $M(t) = |L(t)|^2$, where [19],

$$L(t) = \langle B_-(t)|B_+(t)\rangle = \langle B_0| \, e^{i\hat{H}_- t} e^{-i\hat{H}_+ t} \, |B_0\rangle \ . \tag{3.5}$$

3.1.2.1 Initial bath state

Initial bath state of nanoscale spins bath can be choosen as a tensor product of pure states which is more convinient when compared to mixed states and can be cooked through different techniques [39]. Furthermore, initial bath state dependency can be reduced significantly by dynamical decoupling methods [40]. Consequently, initial spin states can be choosen to be pure coherent spin states (CSS) [41] which are determined by spherical angles $\Omega_i = \theta_i, \phi_i$ so that, for unpolarized and polarized baths we choose spherical angles from uniform distribution and a cone defined by a polar angle θ_p respectively.

For the one-body Hamiltonian given in Eq. (3.2) $L(t)$ can be computed as a product of individual spin propagations. Then, Eq. (3.5) can be re-expressed as,

$$L(t) = \prod_{i=1}^{N} \langle \Omega_i(0)| \, e^{-i2A_i \hat{I}_i^z t} \, |\Omega_i(0)\rangle \,, \tag{3.6}$$

where,

$$|\Omega\rangle = \sum_{m=-I}^{m=I} \binom{2I}{I+m}^{1/2} [\cos(\theta/2)]^{I+m} \, [\sin(\theta/2)]^{I-m} \, e^{-i(I-m)\phi} \, |m\rangle \,. \tag{3.7}$$

from which we can calculate,

$$L(t) = \prod_{i=1}^{N} \Big\{ \sum_{m_i=-I_i}^{I_i} W_i^{m_i} e^{-i2A_i m_i t} \Big\}. \tag{3.8}$$

Here,

$$W_i^{m_i} = \binom{2I_i}{I_i+m_i} [\cos(\theta_i/2)]^{2(I_i+m_i)} \, [\sin(\theta_i/2)]^{2(I_i-m_i)} \,, \tag{3.9}$$

is the weight function which is completely independent from azimuthal angle ϕ, $m \in \{-I, -I+1, \ldots, I-1, I\}$ are the eigenvalues along the quantization axis, θ is the polar angle and the subscript i again denotes the nuclear site index. The simplest case is available for homospin-1/2 environment where Eq. (3.8) reduces to,

$$L(t) = \prod_{i} \Big\{ \cos^2(\theta_i/2) e^{-iA_i t} + \sin^2(\theta_i/2) e^{iA_i t} \Big\}, \tag{3.10}$$

which shares same structure with Eq. (16) derived in [42]. It is also possible to calculate power spectra of LE, $|M(f)|^2$ through the Fourier transform which is given by,

$$M(f) = \sum_{\substack{m_1, m_2, \ldots, m_N, \\ m_1', m_2', \ldots, m_N'}} \Big(\prod_{i=1}^{N} W_i^{m_i} W_i^{m_i'} \Big) \delta \left(f + \frac{1}{\pi} \sum_{i}^{N} A_i (m_i - m_i') \right). \tag{3.11}$$

3.1.3 Effect of quadrupolar interaction to Loschmidt echo

As we mention in the Introduction section we also consider nuclei with $I > 1/2$, and they possess aspherical charge distributions giving rise to a non-zero electric quadrupole moment [43, 44]. These quadrupolar nuclei are affected by the gradient of an electric field that is present at a nuclear site. Such a setting becomes readily available in low-dimensional alloy structures of group III-V semiconductors (like InGaAs quantum dots) arising from the atomistic scale distortions within the tetrahedral bonding of polar constituents [45, 46]. Thus, a quadrupolar NSB has an additional interaction channel described by the Hamiltonian

$$\hat{H}_Q = \sum_i \frac{f_{Qi}}{6} \left\{ 3 \left(\hat{I}_i^z \right)^2 + \frac{\eta_i}{2} \left[\left(\hat{I}_i^+ \right)^2 + \left(\hat{I}_i^- \right)^2 \right] \right\} , \tag{3.12}$$

where, $\hat{I}^{\pm} \equiv \hat{I}^x \pm i\hat{I}^y$ are the standard spin raising/lowering operators, f_{Qi} and η_i, are respectively the quadrupolar frequency and the tensorial electric field gradient biaxiality at the i'th nuclear site, and here we dropped a constant $\hat{I}_i^2$ term [43]. We should note that, QI is not conditioned on the state of central spin, unlike the HFI. So, when both interactions coexist the total Hamiltonian takes the form

$$\hat{H} = \left(\hat{H}_Q + \hat{H}_+ \right) \otimes |\uparrow\rangle \langle\uparrow| + \left(\hat{H}_Q + \hat{H}_- \right) \otimes |\downarrow\rangle \langle\downarrow| . \tag{3.13}$$

3.1.4 Phase flip decoherence

In addition to the above one-body interactions, we would like to consider a generic dephasing channel as well. Qubit decoherence can be calculated via the Lindblad Master equation [47, 48],

$$\frac{\mathrm{d}}{\mathrm{d}t}\hat{\rho}(t) = -i \left[\hat{H}, \hat{\rho}(t) \right] + \sum_{m=1}^{2I} \left[\hat{L}_m \hat{\rho}(t) \hat{L}_m^\dagger - \frac{1}{2} \left\{ \hat{L}_m^\dagger \hat{L}_m, \hat{\rho}(t) \right\} \right] , \tag{3.14}$$

here $\hat{\rho}$ is the density matrix, $[\,,]$ and $\{\,,\}$ represent commutator and anti-commutator, respectively, $\hat{L}_m$ is the Lindblad operator characterizing the nuclear spin's coupling to spin bath. The phase-flip channel can be emloyed for simulating unaccounted, mainly virtual processes in spin-I systems by allowing NSB to

be open as governed by [49, 50]

$$\hat{L}_m = \sqrt{\frac{(2I)!}{m!(2I-m)!}\left(\frac{1-e^{-\gamma}}{2}\right)^m\left(\frac{1+e^{-\gamma}}{2}\right)^{2I-m}}\hat{I}_z^m\,, \tag{3.15}$$

where γ is the phase-flip rate. When this is the case LE can be expressed in terms of spin density matricies $\hat{\rho}^i_{\pm}(t)$ of $(\pm)$ bath trajectories so that LE becomes,

$$M(t) = \prod_{i=1}^{N} \mathrm{Tr}\left(\hat{\rho}^i_-(t)\hat{\rho}^i_+(t)\right)\,, \tag{3.16}$$

where Tr is the trace operator.

3.2 Results

It is possible to observe that for nonthermalized nanoscale NSBs that are coupled to a spin qubit with small deviation in coupling constants A_i, LE can reveal rephase within time since it shows closed system dynamics in short time scales [20]. In pure dephasing model, we show that LE for different NSB or spin length can coalesce to single one. We also consider the nuclear electric quadrupole interaction which is due to atomistic strain in semiconductor matricies for quadrupolar NSBs [45, 46] and reveal under which conditions the QI becomes significant for LE dynamics. Furthermore, we employ phase flip channel to simulate other possible decoherence effects. And finally, we present power spectra of LE for two possible realistic cases of a donor center and a quantum dot which are instances of small and big reservoir respectively.

Throughout this section we use normalized time and frequency, defined by the mean value of uniformly distributed hf coupling constants as, $\bar{A} = \sum_{i=1}^{N} A_i/N$ such that normalized time takes the form $\tilde{t} \equiv t\bar{A}$, and normalized frequency becomes $\tilde{f} \equiv f/\bar{A}$; other normalization schemes also are employed in the literature [15, 37, 51]. The non-zero spread in hf coupling constant is invevitable because of the spatial variation of electron wave function over semiconductor medium. Moreover, we use initial bath state that is consist of tensor product of CSSs

each constructed with polar angle θ_i which distributed uniformly over the interval $[0, \theta_p]$. Therefore, the $\theta_p = \pi$ case corresponds unpolarized nuclear spin environment.

3.2.1 Bath size dependence of LE

As a first example, bath size dependence of LE is employed under mentioned normalization related to mean value of HFI coupling constants. Fig. 3.1 shows LE of spin-1/2 CSSs consist of $N = 1000$ nuclei which are unifromly distributed all over the Bloch sphere initially. The spread in hf coupling constants set to be $0.025\bar{A}$. Altough, this is a small quantity when compared to realistic cases, our purpose here is to show rephasing characteristics[2]. The upper panel of Fig. 3.1 reveals the dephasing in LE and rephasings which are Gaussians of the same halfwidth. Whereas, Fig. 3.1 (bottom) illustrates bath size dependence of LE; observe that larger NSBs shows faster dephasing as experimental studies implies [21]. If the NSB is large enough, rephasing are periodic of the form $\left[\cos\tilde{t}\right]^{\alpha NI}$ with a Gaussian envelope function.

[2]To see the relationship bewteen rephasing amplitude and deviation in HFI coupling constants see Fig. 3.2

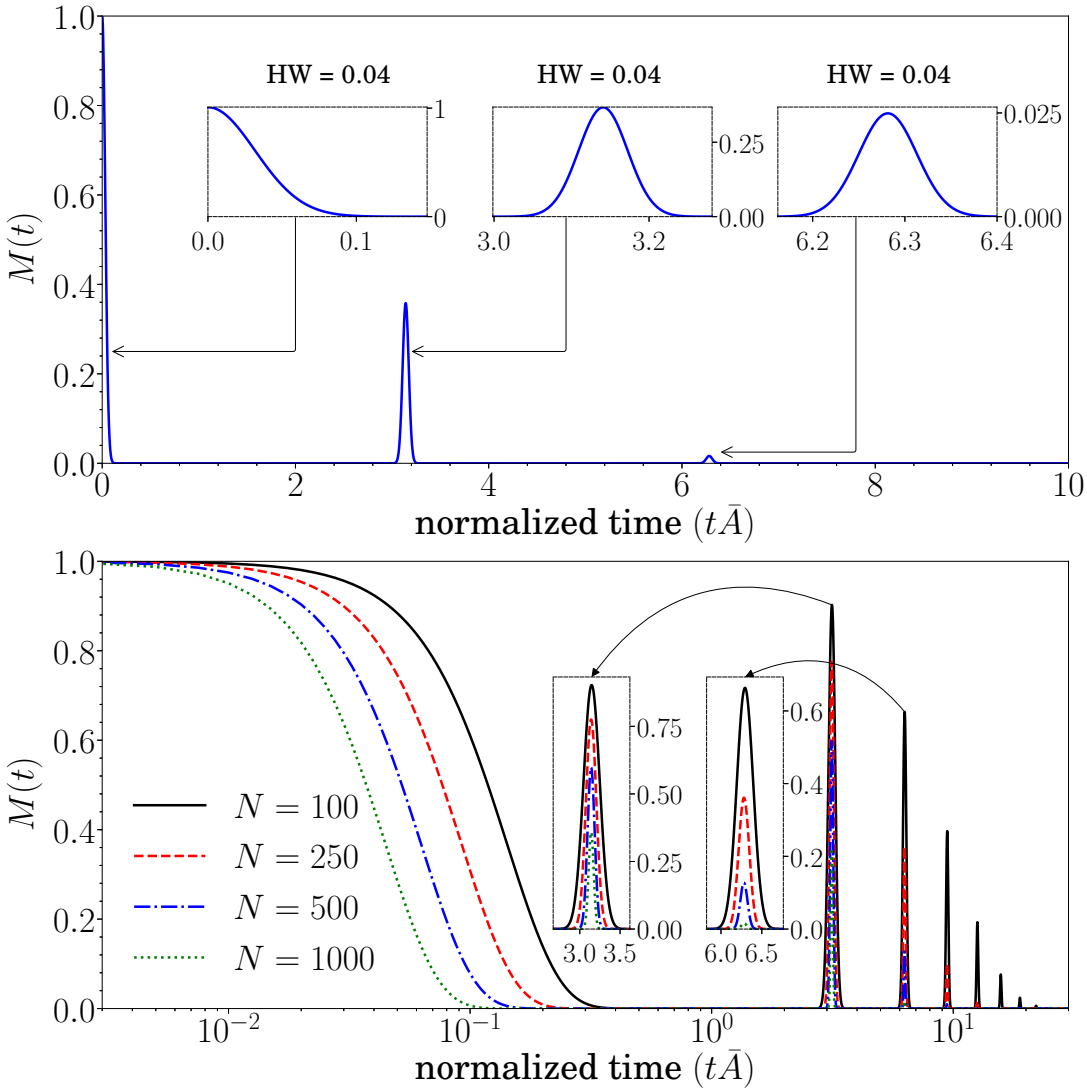

Figure 3.1: (top) LE for $N = 1000$. Insets show the halfwidth (HW) of revivals. (bottom) Effect of different number of nuclear spins, N, forming the bath. In all cases $I = 1/2$, $\Delta A_{max} = 0.025\bar{A}$, initial bath coherent spin states are uniformly distributed over the Bloch sphere.

3.2.2 Effect of bath polarization and hf couplings

Coherence time and rephasing amplitudes are highly initial bath polarization dependent, In Fig. 3.2 (top) we display LE for different initial nuclear spin polarizations which introduce a bias to NSB. The non-vanishing Overhauser Field at $t = 0$ provides longer coherence times in pure dephasing model. It is possible to observe that polarized NSB incorporates stronger rephasing when echo amplitudes and slower decaying Gaussian envelope are considered, consequently. Figure 3.2 (bottom), ΔA_{max} is the maximum deviation from the mean value of HFI constant in NSB (*i.e.* $\Delta A_{max} = \max\{|A_i - \bar{A}|\}$) and individual detuning is added for each nuclear spin site from the uniform distribution. The expression $\left[\cos\tilde{t}\,\right]^{\alpha NI}$ implies that there is no change in width of the first decays since mean value of coupling constants ($\bar{A}$) remains same. However, As HFI constants are chosen to be more resonant, the rephasing amplitudes and number of echoes gets higher exhibiting a similar behavior when compared to the initial spin polarization case.

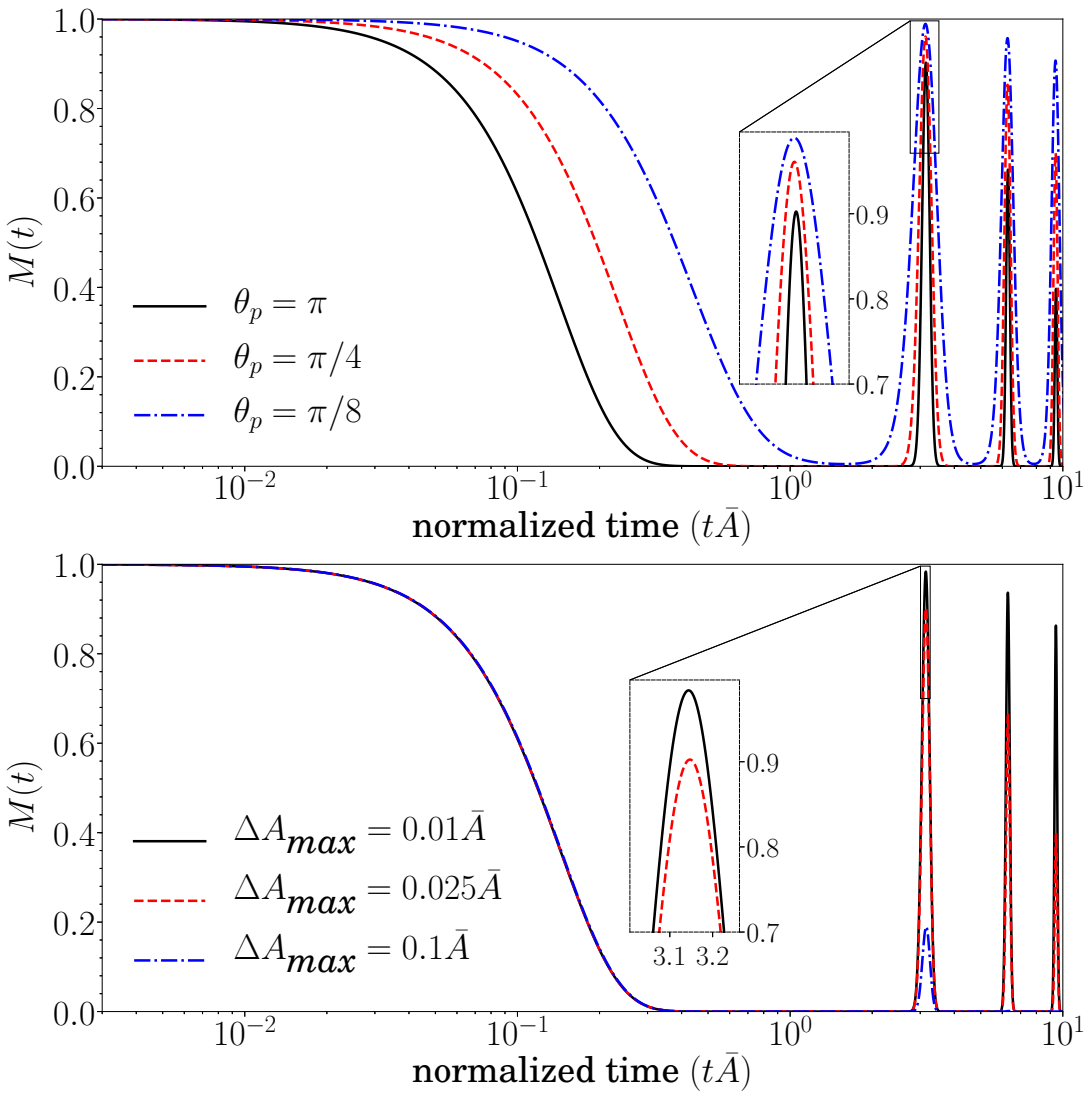

Figure 3.2: (top) Effect of initial nuclear spin polarization (θ_p) on LE, $\Delta A_{max} = 0.025\bar{A}$. (bottom) Effect of spread in the hf coupling constants (ΔA_{max}) of individual nuclear spins; initial bath coherent spin states are uniformly distributed over the Bloch sphere. In all cases $N = 100$, $I = 1/2$.

3.2.3 Spin length dependence

LE can be interpreted as a return probability to a initial bath configuration, since higher spin quantum number (I) deploys more eigenstates, dephasing occurs faster. In Fig. 3.3 (top) we present first decay behavior of LE for different homospin$-I$ environments. When LE is taken into account as a quantum mechanical notion, classical spin baths feature when $I \gg 1$ is satisfied [52, 53]. Whereas, spin-I family of curves can be reduced to single one under the normalization of $t\bar{A}\sqrt{I}$ as in the inset of Fig 3.3. The power spectra of LEs are also given in Fig. 3.3 (bottom) which contains all the necessary information regarding the internal dynamics of dephasing process. Note that here and throughout this thesis we shift power spectra to 0 dB to visualize broadening effect of spin length more clearly. Note that the power spectra widening is also in agreement with temporal behaviour which is proportional to $\sqrt{I}$.

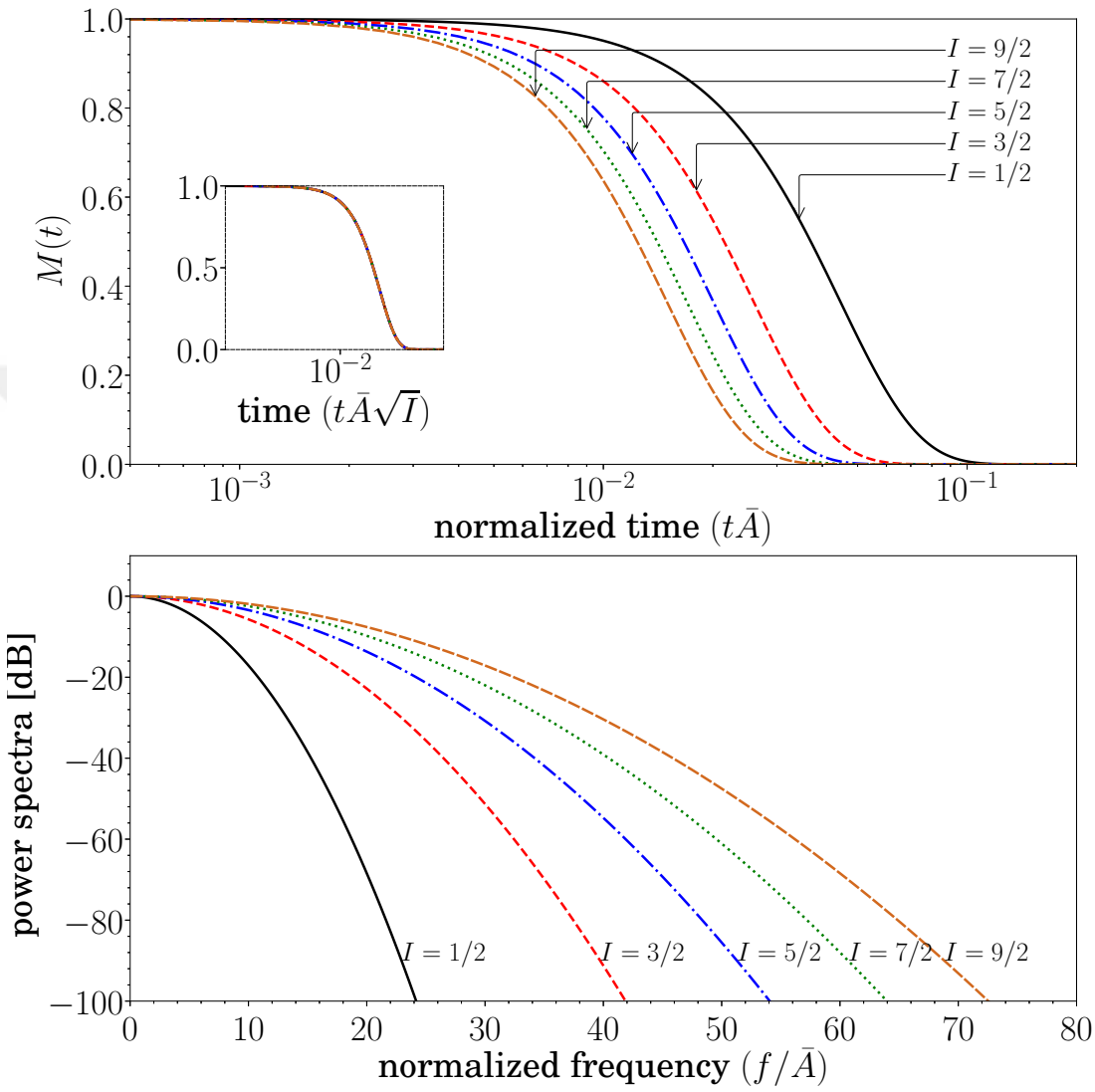

Figure 3.3: Comparison of different spin-I values. (top) Temporal behavior; inset illustrates the coalescence of the family of curves under the indicated normalization. (bottom) spectral behavior. In all cases $N = 1000$, $\Delta A_{max} = 0.25\bar{A}$, and the initial bath spins are uniformly distributed over the Bloch sphere.

An analytical approximated expression of LE for large spin bath limit would be highly desirable, yet it remains as a future work. Cucchietti *e*t al. obtained a derivation for spin-1/2 baths and under some serious assumptions [54]. However, after some numerical analysis we reach to a widely applicable phenomenological

expression that summarizes properties mentioned in previous three subsections which given by,

$$M(\tilde{t}) \sim \exp\left[-NI\left(\alpha_p \sin^2(\tilde{t}) + \beta_p \sigma^2 \tilde{t}^{\,2}\right)\right], \tag{3.17}$$

where σ is the standard deviation of the hf coupling constants, and α_p, β_p, are NSB polarization-dependent fitting parameters. For NSBs that are governed by hf regime, LE curve asymptotically approaches to Eq. (3.17) as long as the number of spins in the environment are increasing without any restriction on spin quantum number, hf coupling spread, etc. Note that it predicts periodicity and rephasing amplitudes correctly especially for $N \gtrsim 1000$ and NI product governs the halfwidth of the first decay, together with the initial bath polarization parameters as covered in Figs. 3.1-3.3.

3.2.4 Quadrupolar interaction

So far, we only included the hf coupling of each nucleus with the central spin (Eq. (3.1)). In the case of quadrupolar NSBs having $I \geq 1$ the QI as described by Eq. (3.12) becomes operative. In Fig. 3.4 the temporal behavior of LE of spin-3/2 and 9/2 NSBs are compared for various mean $\bar{f}_Q = \sum_{i=1}^{N} f_{Qi}/N$ rates from weak to strong coupling limits. We should point out that the QI has a null effect on LE for a nuclear spin under $\eta_i = 0$, i.e., at a *uniaxial* electric field gradient site, or equivalently, its major principal axis aligned with the quantization direction [46]. This is because the $(\hat{I}_i^z)^2$ term in Eq. (3.12) commutes with the $\pm\hat{I}_i^z$ parts of HFI; that is, the fluctuations caused by $(\hat{I}_i^{\pm})^2$ terms are critical, and together with them, the $(\hat{I}_i^z)^2$ term imposes a nontrivial outcome on the dynamics. This necessitates $\eta > 0$, where for alloy quantum dots (like $\mathrm{In}_x\mathrm{Ga}_{1-x}\mathrm{As}$), $\eta \sim 0.2 - 0.6$ [45]. Since η_i term appears in product with f_{Qi} in Eq. (3.12), for simplicity we fix the former to $\eta_i = 0.5$ for all nuclear spins, and let $\Delta f_{Q,max} = 0.2\bar{f}_Q$. The distribution of hf coupling constants is taken as $\Delta A_{max} = 0.25\bar{A}$ that prohibits any revival of LE beyond the initial decay as inferred from Fig. 3.2. In such a practical setting, we first observe that for a given bath size, N, as QI gets stronger it causes a faster decay, and hence broadens the frequency spectrum

of LE. Moreover, the contribution of QI is much more pronounced on polarized NSBs (minding the logarithmic time scale in Fig. 3.4), acting in the direction to depolarize NSB. Furthermore, we note that the significance of QI decreases as the bath size, N, increases. This stems from the fact that the (normalized) first decay rate, $\tilde{f}_{1D}$ as can be extracted from the variance of $M(\tilde{t})$ from Eq. (3.17), has the dependence $\tilde{f}_{1D} \propto \sqrt{NI}$, so that for a given $\bar{f}_Q$, as N increases so does $\tilde{f}_{1D}$, rendering ineffective the QI within the first decay time frame of the LE.

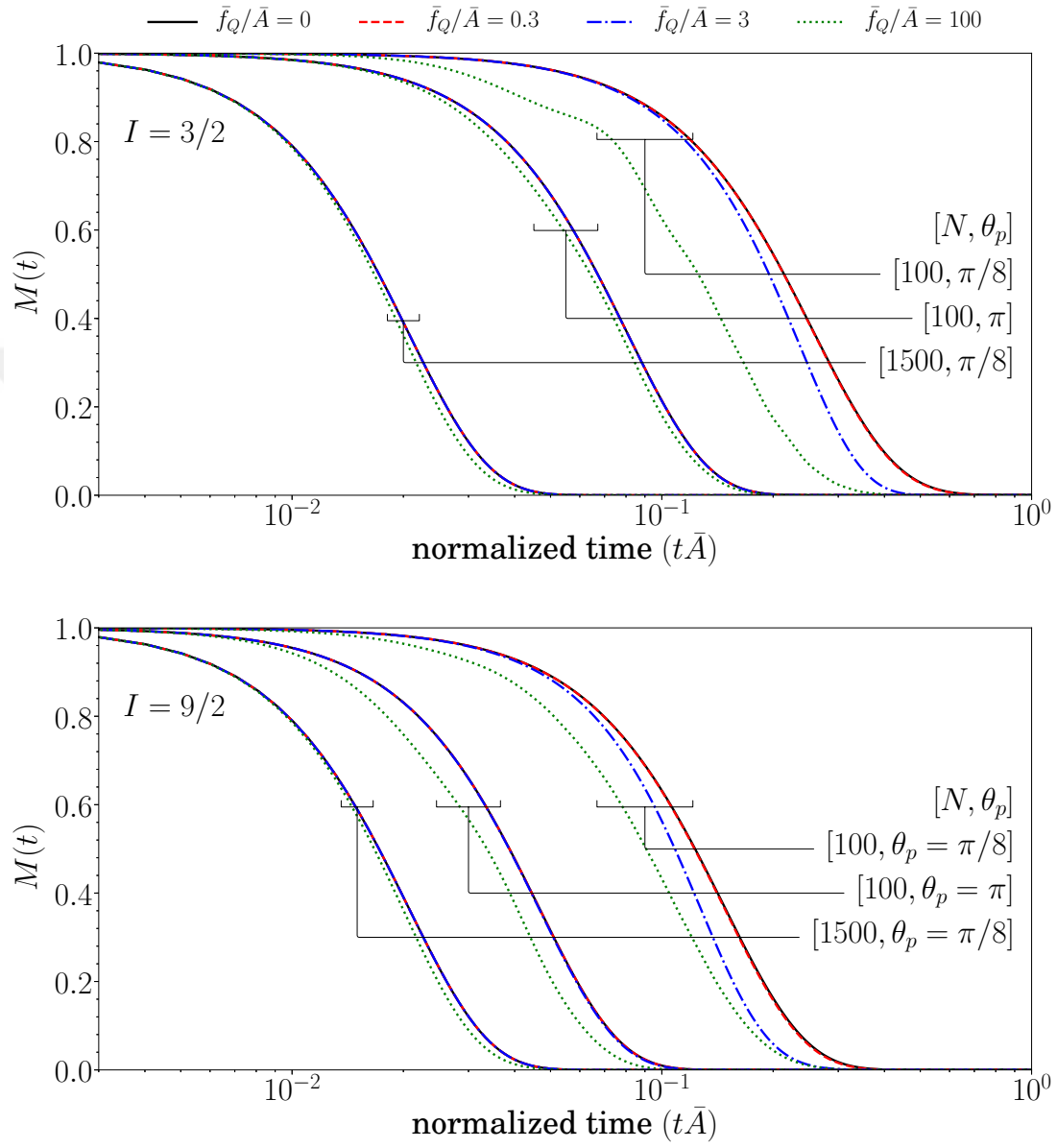

Figure 3.4: Effect of QI on unpolarized ($\theta_p = \pi$) and polarized ($\theta_p = \pi/8$) NSBs, (top) $I = 3/2$, (bottom) $I = 9/2$. For two different N values with $\Delta A_{max} = 0.25\bar{A}$.

3.2.5 Phase flip channel

Before confronting realistic models, other possible decoherence effects can be modelled by introducing phase-flip channel which acts on the off-figonal terms of he density operator. Fig. 3.5 shows both the temporal and spectral behaviour of LE for different phase-flip rates, γ for the spin-1/2 and 3/2. The higher spin-I length makes system more vulnerable to channel and LE's Gaussian profile gains an exponential tail for non-zero phase-flip rate γ. Correspondingly, the power spectra sweeps from Gaussian to Voigt and under strong decoherence limit the Voigt profile becomes a Lorentzian.This agrees with previous works on the deviation from gaussianity under various environmental conditions [55, 20, 56, 57].

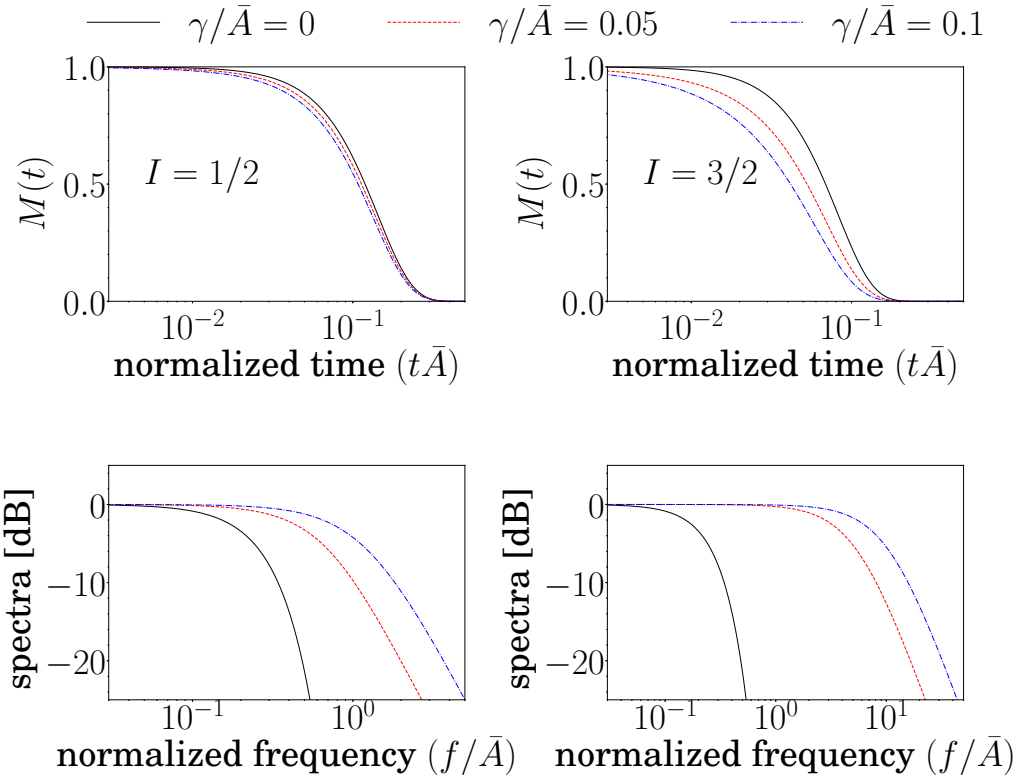

Figure 3.5: Effect of phase flip decoherence, (left) spin-1/2, (right) spin-3/2. $N = 100$, $\Delta A_{max} = 0.3\bar{A}$. Initial bath spins are uniformly distributed over the Bloch sphere.

3.2.6 Realistic solid-state models

After analyzing the NSBs basic traits for LE, we are at the point where the realistic NSBs can be examined. We employ two common NSBs which corresponds small and large reservoir namely, donor/defect center within a semiconductor host matrix, and a lateral quantum dot where the latter represents large NSBs. For an electron which is assumed to be s like state, the slowly varying part of the wave function can be choosen as [51],

$$\Psi(r_i) = \Psi(0) \exp\left(-\frac{r_i^2}{2l_0^2}\right), \tag{3.18}$$

where r_i is the distance of the i'th nuclear site from the origin, and l_0 is the electron confinement radius. In our choice, the NSB constitutes all the nuclei with $|\Psi(r_i)/\Psi(0)| > 10^{-3}$. An effective number of spins N_{eff} can be defined as [10],

$$N_{\mathit{eff}} = \rho \frac{4\pi l_0^3}{3v_0}, \tag{3.19}$$

in terms of the ratio of spinful nuclei, ρ, and the volume occupied by a single atom, v_0, constrained by normalization condition $v_0 \sum_i |\Psi(r_i)|^2 \approx 1$. For 3 dimensional defect center (top) with radius of 5 nm, number of total spins $N_{tot} \approx 25\,000$, number of effective spins $N_{\mathit{eff}} = 100$, the sum of coupling constants can be calculated as, $\sum_{i=1}^{N_{\mathit{eff}}} A_i \approx 0.141$ μeV under the assumption 95% of nuclei in the environment carry spin-0 [55]. For a disk-shaped quantum dot with radius $\rho = 12.5$ nm, height $z = 3$ nm of which the electron envelope wave function taken as uniform in the growth direction, whereas in the radial direction it is taken to be Gaussian, $N_{tot} \approx 70\,000$, $N_{\mathit{eff}} = 10\,000$, $\sum_{i=1}^{N_{tot}} A_i \approx 82$ μeV, the sum of couplings estimated as $\sum_{i=1}^{N_{\mathit{eff}}} A_i \approx 70.856$ μeV.

Power spectra of LE for both defect center and quantum dot are considered in Fig. 3.6 under different set of parameters which are all agreement with NSB properties addressed in previous subsection. To begin with, the polarized bath dramatically narrows the frequency spectrum. The observation of $\sqrt{I}$ broadening still valid when spin-1/2,3/2,9/2 environments compared. Furthermore, the frequency bandwidth of donor center is two orders of magnitude narrower than comared to quantum dot case where the latter is about hundreds of megahertz.

This situation is directly related to Eq. (3.17). Regarding QI, the quadrupolar frequency dictated by strain is typically in the range $f_Q \sim 2$–8 MHz for typical quantum dots [45], and 3–6 MHz for defect centers, as in hexagonal BN flakes [58]. In our examples here, the mean hf coupling constant, $\bar{A}$ is about 0.34 MHz (1.7 MHz) for the donor center (quantum dot), so as a representative value we consider $\bar{f}_Q/\bar{A} = 10$, along with $\eta_i = 0.5$. From Fig. 3.6 it can be seen that QI is ineffective on LE for a large quantum dot, whereas it leaves its mark in the donor center with polarized NSB having a small NI product, in parallel to our conclusions from Fig. 3.4 and Eq. (3.17).

Finally, we would like to comment on the utility of such power spectra as in Fig. 3.6. In simple terms, they specify the characteristic bandwidth of HFI and QI fluctuations in relation to the qubit coherence. As such, this may help to assess the efficacy of the dynamical decoupling techniques [40]. In a more specific context, the spectrum of NSB hf fluctuations plays a crucial role in the recently discovered hf-mediated electric dipole spin resonance, in the form of both driving and detuning it [59, 60].

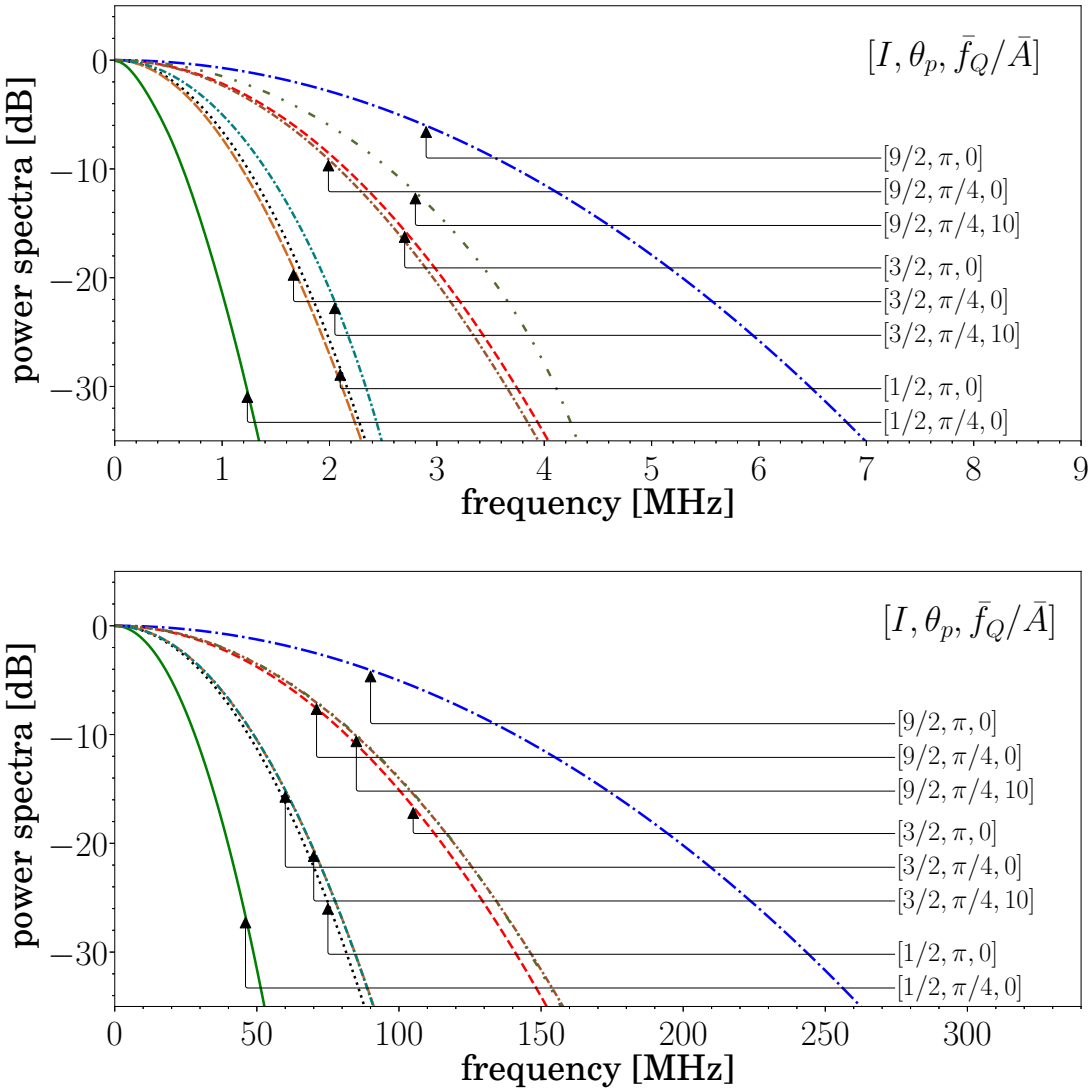

Figure 3.6: Power spectra of LE for realistic systems under different spin-I, polarization (θ_p) and quadrupolar frequencies ($\bar{f}_Q$). (top) donor center, $N_{eff} = 100$, (bottom) lateral quantum dot, $N_{eff} = 10\ 000$. For the bottom case, $\bar{f}_Q/\bar{A}$=0, 10 curves become indiscernible for each I.

Chapter 4

Conclusions and future work

In nanoscale spin bath the analysis of spin decoherence is important for various purposes in quantum technologies [27, 61, 62]. This thesis first gives a basic recipe for deducing LE by JW diagonalization both for uniform and site dependently-interacting spin chains. Then, uncovers the characteristic effects of key parameters to *non*-interacting NSBs like size, initial polarization, coupling inhomogeneity, spin quantum number, and offers a phenomenological expression of LE in the pure dephasing regime.

Additionally, the effect of QI on LE is taken into account for the quadrupolar nuclei which are prevalent in III-V semiconductors. In particular, it is the QI biaxiality term that has important ramifications on the qubit decoherence. From the moderate coupling regime onwards ($\bar{f}_Q \gtrsim \bar{A}$), QI causes a faster decay of initial coherence that gets more pronounced for polarized and small NI-product NSBs. Furthermore, phase-flip channel is studied to see vulnerability of spin-I environments especially when $I \gg 1$. Lastly, we contrasted two realistic cases of a donor center and a quantum dot representing small and large NSBs, respectively. Here, for quantum dots with $N \gtrsim 10\ 000$ nuclear spins, the LE spectrum can stretch to 100 MHz range, and the effect of QI is rather negligible. On the other hand for donor centers, as this width narrows down by more than an order of magnitude both the dynamical decoupling techniques become feasible, and the

QI begins to show its presence.

It remains as a future work to discover long term dynamics in a detailed way where intrabath interactions also becomes crucial, that can be compared with the experimental results in the literature [63]. As a matter of fact, there are specialized techniques for handling the large interacting NSBs like cluster-correlation expansion [64, 61] which can be compared with exact solutions like the ones derived in second chapter.

Bibliography

[1] P. C. Maurer, G. Kucsko, C. Latta, L. Jiang, N. Y. Yao, S. D. Bennett, F. Pastawski, D. Hunger, N. Chisholm, M. Markham, D. J. Twitchen, J. I. Cirac, and M. D. Lukin, "Room-temperature quantum bit memory exceeding one second," *Science*, vol. 336, no. 6086, pp. 1283–1286, 2012.

[2] J. M. Taylor, C. M. Marcus, and M. D. Lukin, "Long-lived memory for mesoscopic quantum bits," *Phys. Rev. Lett.*, vol. 90, p. 206803, May 2003.

[3] J. M. Taylor, A. İmamoğlu, and M. D. Lukin, "Controlling a mesoscopic spin environment by quantum bit manipulation," *Phys. Rev. Lett.*, vol. 91, p. 246802, Dec 2003.

[4] W. M. Witzel and S. Das Sarma, "Nuclear spins as quantum memory in semiconductor nanostructures," *Phys. Rev. B*, vol. 76, p. 045218, Jul 2007.

[5] J. Taylor, G. Giedke, H. Christ, B. Paredes, J. Cirac, P. Zoller, M. Lukin, and A. İmamoğlu, "Quantum information processing using localized ensembles of nuclear spins," *arXiv preprint cond-mat/0407640*, 2004.

[6] J. Casanova, Z.-Y. Wang, and M. B. Plenio, "Arbitrary nuclear-spin gates in diamond mediated by a nitrogen-vacancy-center electron spin," *Phys. Rev. A*, vol. 96, p. 032314, Sep 2017.

[7] D. Loss and D. P. DiVincenzo, "Quantum computation with quantum dots," *Phys. Rev. A*, vol. 57, pp. 120–126, Jan 1998.

[8] A. İmamoğlu, D. D. Awschalom, G. Burkard, D. P. DiVincenzo, D. Loss, M. Sherwin, and A. Small, "Quantum information processing using quantum dot spins and cavity qed," *Phys. Rev. Lett.*, vol. 83, pp. 4204–4207, Nov 1999.

[9] I. A. Merkulov, A. L. Efros, and M. Rosen, "Electron spin relaxation by nuclei in semiconductor quantum dots," *Phys. Rev. B*, vol. 65, p. 205309, Apr 2002.

[10] J. Schliemann, A. Khaetskii, and D. Loss, "Electron spin dynamics in quantum dots and related nanostructures due to hyperfine interaction with nuclei," *Journal of Physics: Condensed Matter*, vol. 15, no. 50, p. R1809, 2003.

[11] W. Zhang, V. V. Dobrovitski, K. A. Al-Hassanieh, E. Dagotto, and B. N. Harmon, "Hyperfine interaction induced decoherence of electron spins in quantum dots," *Phys. Rev. B*, vol. 74, p. 205313, Nov 2006.

[12] C. Latta, A. Srivastava, and A. İmamoğlu, "Hyperfine interaction-dominated dynamics of nuclear spins in self-assembled ingaas quantum dots," *Phys. Rev. Lett.*, vol. 107, p. 167401, Oct 2011.

[13] M. Gaudin, "Diagonalisation d'une classe d'hamiltoniens de spin," *Journal de Physique*, vol. 37, no. 10, pp. 1087–1098, 1976.

[14] E. Barnes, L. Cywiński, and S. Das Sarma, "Nonperturbative master equation solution of central spin dephasing dynamics," *Phys. Rev. Lett.*, vol. 109, p. 140403, Oct 2012.

[15] D. Stanek, C. Raas, and G. S. Uhrig, "Dynamics and decoherence in the central spin model in the low-field limit," *Phys. Rev. B*, vol. 88, p. 155305, Oct 2013.

[16] K. A. Al-Hassanieh, V. V. Dobrovitski, E. Dagotto, and B. N. Harmon, "Numerical modeling of the central spin problem using the spin-coherent-state p representation," *Phys. Rev. Lett.*, vol. 97, p. 037204, Jul 2006.

[17] H. Christ, J. I. Cirac, and G. Giedke, "Entanglement generation via a completely mixed nuclear spin bath," *Phys. Rev. B*, vol. 78, p. 125314, Sep 2008.

[18] H. Schwager, J. I. Cirac, and G. Giedke, "Interfacing nuclear spins in quantum dots to a cavity or traveling-wave fields," *New Journal of Physics*, vol. 12, no. 4, p. 043026, 2010.

[19] R. A. Jalabert and H. M. Pastawski, "Environment-independent decoherence rate in classically chaotic systems," *Phys. Rev. Lett.*, vol. 86, pp. 2490–2493, Mar 2001.

[20] W. Yao, R.-B. Liu, and L. J. Sham, "Restoring coherence lost to a slow interacting mesoscopic spin bath," *Phys. Rev. Lett.*, vol. 98, p. 077602, Feb 2007.

[21] L. Buljubasich, C. M. Sánchez, A. D. Dente, P. R. Levstein, A. K. Chattah, and H. M. Pastawski, "Experimental quantification of decoherence via the loschmidt echo in a many spin system with scaled dipolar hamiltonians," *The Journal of Chemical Physics*, vol. 143, no. 16, p. 164308, 2015.

[22] C. M. Sánchez, P. R. Levstein, L. Buljubasich, H. M. Pastawski, and A. K. Chattah, "Quantum dynamics of excitations and decoherence in many-spin systems detected with loschmidt echoes: its relation to their spreading through the hilbert space," *Philosophical Transactions of the Royal Society of London A: Mathematical, Physical and Engineering Sciences*, vol. 374, no. 2069, 2016.

[23] C. Deng and X. Hu, "Decoherence of nuclear spin quantum memory in a quantum dot," *IEEE Transactions on Nanotechnology*, vol. 4, pp. 35–39, Jan 2005.

[24] L. Cywiński, W. M. Witzel, and S. Das Sarma, "Electron spin dephasing due to hyperfine interactions with a nuclear spin bath," *Phys. Rev. Lett.*, vol. 102, p. 057601, Feb 2009.

[25] I. A. Merkulov, G. Alvarez, D. R. Yakovlev, and T. C. Schulthess, "Long-term dynamics of the electron-nuclear spin system of a semiconductor quantum dot," *Phys. Rev. B*, vol. 81, p. 115107, Mar 2010.

[26] W. Yao, R.-B. Liu, and L. J. Sham, "Theory of electron spin decoherence by interacting nuclear spins in a quantum dot," *Phys. Rev. B*, vol. 74, p. 195301, Nov 2006.

[27] C. Deng and X. Hu, "Analytical solution of electron spin decoherence through hyperfine interaction in a quantum dot," *Phys. Rev. B*, vol. 73, p. 241303, Jun 2006.

[28] W. M. Witzel and S. Das Sarma, "Quantum theory for electron spin decoherence induced by nuclear spin dynamics in semiconductor quantum computer architectures: Spectral diffusion of localized electron spins in the nuclear solid-state environment," *Phys. Rev. B*, vol. 74, p. 035322, Jul 2006.

[29] M. H. Levitt, *Spin dynamics: basics of nuclear magnetic resonance*. John Wiley & Sons, 2007.

[30] P. Coleman, *Introduction to Many-Body Physics*. Cambridge University Press, 2015.

[31] Z. Huang, G. Sadiek, and S. Kais, "Time evolution of a single spin inhomogeneously coupled to an interacting spin environment," *The Journal of Chemical Physics*, vol. 124, no. 14, p. 144513, 2006.

[32] E. Lieb, T. Schultz, and D. Mattis, "Two soluble models of an antiferromagnetic chain," *Annals of Physics*, vol. 16, no. 3, pp. 407 – 466, 1961.

[33] D. Rossini, T. Calarco, V. Giovannetti, S. Montangero, and R. Fazio, "Decoherence induced by interacting quantum spin baths," *Phys. Rev. A*, vol. 75, p. 032333, Mar 2007.

[34] S. Sharma, V. Mukherjee, and A. Dutta, "Study of loschmidt echo for a qubit coupled to an xy-spin chain environment," *The European Physical Journal B*, vol. 85, p. 143, Apr 2012.

[35] M. Zhong and P. Tong, "Loschmidt echo of a two-level qubit coupled to nonuniform anisotropic xy chains in a transverse field," *Phys. Rev. A*, vol. 84, p. 052105, Nov 2011.

[36] C. Cormick and J. Pablo Paz, "Decoherence induced by a dynamic spin environment: The universal regime," *Phys. Rev. A*, vol. 77, p. 022317, Feb 2008.

[37] D. Stanek, C. Raas, and G. S. Uhrig, "From quantum-mechanical to classical dynamics in the central-spin model," *Phys. Rev. B*, vol. 90, p. 064301, Aug 2014.

[38] E. Taha Güldeste and C. Bulutay, "Hyperfine and electric quadrupole interaction-driven Loschmidt echo in nanoscale nuclear spin baths," *to be published by Phys. Rev. B; arXiv:1804.07219*, Apr. 2018.

[39] G. Giedke, J. M. Taylor, D. D'Alessandro, M. D. Lukin, and A. İmamoğlu, "Quantum measurement of a mesoscopic spin ensemble," *Phys. Rev. A*, vol. 74, p. 032316, Sep 2006.

[40] D. Suter and G. A. Álvarez, "*Colloquium* : Protecting quantum information against environmental noise," *Rev. Mod. Phys.*, vol. 88, p. 041001, Oct 2016.

[41] J. Ma, X. Wang, C. P. Sun, and F. Nori, "Quantum spin squeezing," *Phys. Rep.*, vol. 509, no. 2?3, pp. 89 – 165, 2011.

[42] F. M. Cucchietti, J. P. Paz, and W. H. Zurek, "Decoherence from spin environments," *Phys. Rev. A*, vol. 72, p. 052113, Nov 2005.

[43] M. Cohen and F. Reif, "Quadrupole effects in nuclear magnetic resonance studies of solids," vol. 5 of *Solid State Physics*, pp. 321 – 438, Academic Press, 1957.

[44] T. Das and E. Hahn, *Nuclear Quadrupole Resonance Spectroscopy*. Solid state physics. Suppl, Academic Press, 1964.

[45] C. Bulutay, "Quadrupolar spectra of nuclear spins in strained ingaas quantum dots," *Phys. Rev. B*, vol. 85, p. 115313, Mar 2012.

[46] C. Bulutay, E. A. Chekhovich, and A. I. Tartakovskii, "Nuclear magnetic resonance inverse spectra of ingaas quantum dots: Atomistic level structural information," *Phys. Rev. B*, vol. 90, p. 205425, Nov 2014.

[47] J. R. Johansson, P. D. Nation, and F. Nori, "Qutip: An open-source python framework for the dynamics of open quantum systems," *Comput. Phys. Commun.*, vol. 183, pp. 1760–1772, 2012.

[48] J. R. Johansson, P. D. Nation, and F. Nori, "Qutip2:a python framework for the dynamics of open quantum systems," *Comput. Phys. Commun.*, vol. 184, pp. 1234–1240, 2013.

[49] S. Pirandola, S. Mancini, S. L. Braunstein, and D. Vitali, "Minimal qudit code for a qubit in the phase-damping channel," *Phys. Rev. A*, vol. 77, p. 032309, Mar 2008.

[50] C. Bulutay, "Cat-state generation and stabilization for a nuclear spin through electric quadrupole interaction," *Phys. Rev. A*, vol. 96, p. 012312, Jul 2017.

[51] J. Hackmann and F. B. Anders, "Spin noise in the anisotropic central spin model," *Phys. Rev. B*, vol. 89, p. 045317, Jan 2014.

[52] M. Y. Petrov and S. Yakovlev, "Comparison of quantum-mechanical and semiclassical approaches for an analysis of spin dynamics in quantum dots," *Journal of Experimental and Theoretical Physics*, vol. 115, no. 2, pp. 326–336, 2012.

[53] T. Opatrný, "Squeezing with classical hamiltonians," *Phys. Rev. A*, vol. 92, p. 033801, Sep 2015.

[54] F. Cucchietti, S. Fernandez-Vidal, and J. P. Paz, "Universal decoherence induced by an environmental quantum phase transition," *Phys. Rev. A*, vol. 75, p. 032337, Mar 2007.

[55] W. A. Coish and D. Loss, "Hyperfine interaction in a quantum dot: Non-markovian electron spin dynamics," *Phys. Rev. B*, vol. 70, p. 195340, Nov 2004.

[56] C. Cormick and J. P. Paz, "Decoherence induced by a dynamic spin environment: The universal regime," *Phys. Rev. A*, vol. 77, p. 022317, Feb 2008.

[57] W. A. Coish, J. Fischer, and D. Loss, "Free-induction decay and envelope modulations in a narrowed nuclear spin bath," *Phys. Rev. B*, vol. 81, p. 165315, Apr 2010.

[58] W. A. Coish and D. Loss, "Hyperfine interaction in a quantum dot: Non-markovian electron spin dynamics," *Phys. Rev. B*, vol. 70, p. 195340, Nov 2004.

[59] E. A. Laird, C. Barthel, E. I. Rashba, C. M. Marcus, M. P. Hanson, and A. C. Gossard, "Hyperfine-mediated gate-driven electron spin resonance," *Phys. Rev. Lett.*, vol. 99, p. 246601, Dec 2007.

[60] E. I. Rashba, "Theory of electric dipole spin resonance in quantum dots: Mean field theory with gaussian fluctuations and beyond," *Phys. Rev. B*, vol. 78, p. 195302, Nov 2008.

[61] W. Yang, W.-L. Ma, and R.-B. Liu, "Quantum many-body theory for electron spin decoherence in nanoscale nuclear spin baths," *Reports on Progress in Physics*, vol. 80, no. 1, p. 016001, 2017.

[62] R. N. E. Malein, T. S. Santana, J. M. Zajac, A. C. Dada, E. M. Gauger, P. M. Petroff, J. Y. Lim, J. D. Song, and B. D. Gerardot, "Screening nuclear field fluctuations in quantum dots for indistinguishable photon generation," *Phys. Rev. Lett.*, vol. 116, p. 257401, Jun 2016.

[63] M. J. Stanley, C. Matthiesen, J. Hansom, C. Le Gall, C. H. H. Schulte, E. Clarke, and M. Atatüre, "Dynamics of a mesoscopic nuclear spin ensemble interacting with an optically driven electron spin," *Phys. Rev. B*, vol. 90, p. 195305, Nov 2014.

[64] W. Yang and R.-B. Liu, "Quantum many-body theory of qubit decoherence in a finite-size spin bath," *Phys. Rev. B*, vol. 78, p. 085315, Aug 2008.

Appendix A

Derivations relevant to Jordan-Wigner transformation

A.1 Coupled equations

Let's have a look at commutation, $[\eta_k, H]$

$$\begin{aligned}
[\eta_k, H] &= \eta_k H - H\eta_k \\
&= \sum_{k'} \Lambda_{k'} \eta_k \eta^\dagger_{k'} \eta_{k'} - \sum_{k'} \Lambda_{k'} \eta^\dagger_{k'} \eta_{k'} \eta_k \\
&= \sum_{k'} \Lambda_{k'} (\delta_{kk'} - \eta^\dagger_{k'} \eta_k) \eta_{k'} - \sum_{k'} \Lambda_{k'} \eta^\dagger_{k'} \eta_{k'} \eta_k \\
&= \sum_{k'} \Lambda_{k'} \delta_{kk'} \eta_{k'} \\
&= \Lambda_k \eta_k
\end{aligned} \tag{A.1}$$

Using the relation above with (2.22) and (2.27),

$$\begin{aligned}
[\eta_k, H] = &\sum_n (g_{kn} c_n + h_{kn} c^\dagger_n) \Big[\sum_{i,j} (c^\dagger_i A_{ij} c_i) + \frac{1}{2} (c^\dagger_i B_{ij} c^\dagger_j + c_j B_{ji} c_i) \Big] \\
&- \Big[\sum_{i,j} (c^\dagger_i A_{ij} c_i) + \frac{1}{2} (c^\dagger_i B_{ij} c^\dagger_j + c_j B_{ji} c_i) \Big] \sum_n (g_{kn} c_n + h_{kn} c^\dagger_n)
\end{aligned} \tag{A.2}$$

$$
\begin{aligned}
&= \sum_{i,j,n} \Big\{ g_{kn} (\overbrace{c_n c_i^\dagger}^{\delta_{ni} - c_i^\dagger c_n} A_{ij} c_j - c_i^\dagger A_{ij} c_j c_n) \\
&\quad + \frac{g_{kn}}{2} (\overbrace{c_n c_i^\dagger}^{\delta_{ni} - c_i^\dagger c_n} B_{ij} c_j^\dagger - c_i^\dagger B_{ij} c_j^\dagger c_n) \\
&\quad + \frac{g_{kn}}{2} (\overbrace{c_n c_j}^{-c_j c_n} B_{ji} c_i - c_j B_{ji} c_i c_n) \\
&\quad + \frac{h_{kn}}{2} (\overbrace{c_n^\dagger c_i^\dagger}^{-c_i^\dagger c_n^\dagger} A_{ij} c_j - c_i^\dagger A_{ij} c_j c_n) \\
&\quad + \frac{h_{kn}}{2} (\overbrace{c_n^\dagger c_i^\dagger}^{-c_i^\dagger c_n^\dagger} B_{ij} c_j^\dagger - c_i^\dagger B_{ij} c_j^\dagger c_n^\dagger) \\
&\quad + \frac{h_{kn}}{2} (\overbrace{c_n^\dagger c_j}^{\delta_{nj} - c_j c_n^\dagger} B_{ji} c_i - c_j B_{ji} c_i c_n^\dagger) \Big\} \qquad \text{(A.3)} \\
&= \sum_{i,j,n} \Big\{ g_{kn} (A_{ij} c_j \delta_{ni} - c_i^\dagger A_{ij} (\overbrace{c_n c_j + c_j c_n}^{0})) \\
&\quad + \frac{g_{kn}}{2} (B_{ij} c_j^\dagger \delta_{ni} - c_i^\dagger B_{ij} (\overbrace{c_n c_j^\dagger + c_j^\dagger c_n}^{\delta_{nj}})) \\
&\quad + \frac{g_{kn}}{2} (-B_{ji} c_j (\overbrace{c_n c_i + c_i c_n}^{0})) \\
&\quad + h_{kn} (-A_{ij} c_i^\dagger (\overbrace{c_n^\dagger c_j + c_j c_n^\dagger}^{\delta_{ij}})) \\
&\quad + \frac{h_{kn}}{2} (-B_{ij} c_i^\dagger (\overbrace{c_n^\dagger c_j^\dagger + c_j^\dagger c_i^\dagger}^{0})) \\
&\quad + \frac{h_{kn}}{2} (B_{ji} c_i \delta_{nj} - c_j B_{ji} (\overbrace{c_n^\dagger c_i + c_i c_n^\dagger}^{\delta_{ni}})) \Big\} = \Lambda_k \sum_n (g_{kn} c_n + h_{kn} c_n^+). \qquad \text{(A.4)}
\end{aligned}
$$

Here, we obviously used anticommutation relations for fermions. Equating like terms and rearranging indicies of A and B matrices[1] yields following coupled

[1]Here we used symmetric and anti-symmetric properties of A and B matrices.

equations,

$$\Lambda_k g_{kn} = \sum_i (g_{ki} A_{in} - h_{ki} B_{in}), \tag{A.5}$$

$$\Lambda_k h_{kn} = \sum_i (g_{ki} B_{in} - h_{ki} A_{in}). \tag{A.6}$$

A.2 Constraints for η_k and $\eta_k^\dagger$ to be cannonical

Considering that η_k^+, η_n^+ to be canonical

$$\begin{aligned}
[\eta_k, \eta_n]_+ &= \eta_k \eta_n + \eta_n \eta_k = 0 \\
&= \sum_i (g_{ki} c_i + h_{ki} c_i^\dagger) \sum_j (g_{nj} c_j + h_{nj} c_j^\dagger) \\
&+ \sum_j (g_{nj} c_j + h_{nj} c_j^\dagger) \sum_i (g_{ki} c_i + h_{ki} c_i^\dagger) \\
&= \sum_{ij} (g_{ki} g_{nj} c_i c_j + g_{ki} h_{nj} c_i c_j^\dagger) \\
&+ \sum_{ij} (h_{ki} g_{nj} c_i^\dagger c_j + h_{ki} h_{nj} c_i^\dagger c_j^\dagger) \\
&+ \sum_{ij} (g_{ki} g_{nj} c_j c_i + g_{ki} h_{nj} c_j^\dagger c_i) \\
&+ \sum_{ij} (h_{ki} g_{nj} c_j c_i^\dagger + h_{ki} h_{nj} c_j^\dagger c_i^\dagger) \\
&= \sum_{ij} (g_{ki} g_{nj} [c_i, c_j]_+ + h_{ki} h_{nj} [c_i^\dagger, c_j^\dagger]_+) \\
&+ \sum_{ij} (g_{ki} h_{nj} [c_i, c_j^\dagger]_+ + h_{ki} g_{nj} [c_j, c_i^\dagger]).
\end{aligned}$$

Yielding,

$$\sum_i (g_{ki} h_{ni} + h_{ki} g_{ni}) = 0. \tag{A.7}$$

Similarly, one can deduce,

$$\sum_i (g_{ki} g_{ni} + h_{ki} h_{ni}) = \delta_{ij}, \tag{A.8}$$

from $[\eta_k, \eta_n^\dagger]_+ = \delta_{nk}$. (2.33) and (2.34) are two constraints that needs to be satisfied for canonical operators η_k, $\eta_k^\dagger$.

A.3 Elements of G Matrix

Let's write, matrix elements of $U^{(g)}U^{(e)-1}$ as,

$$U^{(g)}U^{(e)-1} = \begin{pmatrix} r & q \\ q* & r* \end{pmatrix}. \tag{A.9}$$

Connecting excited and ground state operators,

$$\eta_k^{(g)} = \sum_i (r_{ki}\eta_i^{(e)} + q_{ki}\eta_i^{\dagger(e)}) \tag{A.10}$$

Observe that $\eta_k|B^{(g)}\rangle = 0$. Then,

$$\begin{aligned}
\eta_k|B^{(g)}\rangle &= \sum_i (r_{ki}\eta_i^{(e)} + q_{ki}\eta_i^{\dagger(e)}) e^{(1/2\sum_{n,m}\eta_n^{\dagger(e)}G_{nm}\eta_m^{\dagger(e)})}|B^{(e)}\rangle = 0 \\
&= \sum_i (r_{ki}\eta_i^{(e)} + q_{ki}\eta_i^{\dagger(e)}) \prod_{n,m}\Big[1 + \frac{1}{2}G_{nm}\eta_n^{\dagger(e)}\eta_m^{\dagger(e)} + \frac{1}{8}(G_{nm}\eta_n^{\dagger(e)}\eta_m^{\dagger(e)})^2 + \dots\Big]|B^{(e)}\rangle \\
&= \sum_i \prod_{n,m} (r_{ki}\eta_i^{(e)} + q_{ki}\eta_i^{\dagger(e)})\Big[1 + \frac{1}{2}G_{nm}\eta_n^{\dagger(e)}\eta_m^{\dagger(e)}\Big]|B^{(e)}\rangle \\
&= \prod_{n,m}\Big[\sum_i r_{ki}\eta_i^{(e)} + \sum_i q_{ki}\eta_i^{\dagger(e)} \\
&+ \frac{1}{2}\sum_i r_{ki}\eta_i^{(e)}G_{nm}\eta_n^{\dagger(e)}\eta^{\dagger(e)} + \frac{1}{2}\sum_i q_{ki}\eta_i^{\dagger(e)}G_{nm}\eta_n^{\dagger(e)}\eta^{\dagger(e)}\Big]|B^{(e)}\rangle \\
&= \prod_{n,m}\Big[\sum_i q_{ki}\eta_i^{\dagger(e)} + \frac{1}{2}\sum_i r_{ki}\eta_i^{(e)}G_{nm}\eta_n^{\dagger(e)}\eta_m^{\dagger(e)}\Big]|B^{(e)}\rangle \\
&= \prod_{n,m}\Big[\sum_i q_{ki}\eta_i^{\dagger(e)} + \frac{1}{2}\sum_i r_{ki}\eta_i^{(e)}G_{nm}\eta_n^{\dagger(e)}\eta_m^{\dagger(e)}\Big]|B^{(e)}\rangle \\
&= \prod_{n,m}\Big[\sum_i q_{ki}\eta_i^{\dagger(e)} + \frac{1}{2}\sum_i r_{ki}G_{nm}(\delta_{in} - \eta_n^{\dagger(e)}\eta_i^{(e)})\eta_m^{\dagger(e)}\Big]|B^{(e)}\rangle \\
&= \prod_{n,m}\Big[\sum_i q_{ki}\eta_i^{\dagger(e)} + \frac{1}{2}\sum_i r_{ki}G_{nm}(\delta_{in}\eta_m^{\dagger(e)} - \eta_n^{\dagger(e)}\eta_i^{(e)}\eta_m^{\dagger(e)})\Big]|B^{(e)}\rangle \\
&= \prod_{n,m}\Big[\sum_i q_{ki}\eta_i^{\dagger(e)} + \frac{1}{2}\sum_i r_{ki}G_{nm}(\delta_{in}\eta_m^{\dagger(e)} - \eta_n^{\dagger(e)}(\delta_{im} - \eta_m^{\dagger(e)}\eta_i^{(e)}))\Big]|B^{(e)}\rangle \\
&= \prod_{n,m}\Big[\sum_i q_{ki}\eta_i^{\dagger(e)} + \frac{1}{2}\sum_i r_{ki}G_{nm}(\delta_{in}\eta_m^{\dagger(e)} - \eta_n^{\dagger(e)}\delta_{im})\Big]|B^{(e)}\rangle
\end{aligned}$$

Then, collecting coefficients of like terms yields the following equation,

$$q_{km} + \sum_i r_{ki}G_{im} = 0, \tag{A.11}$$

which one can find elements of G.

A.4 Derivation of generalized expression for Loschmidt echo

The overlap of ground and excited states can be written as,

$$\langle B^{(g)}(t)|B^{(e)}(t)\rangle = \frac{1}{\Upsilon^2}\langle B^{(e)}|e^{(1/2\sum_{n,m}\eta_n^{(e)}G^*_{nm}\eta_m^{(e)})}e^{iE_0t}e^{-iH^{(e)}}e^{(1/2\sum_{i,j}\eta_i^{\dagger(e)}G^\dagger_{ij}\eta_j^{\dagger(e)})}|B^{(e)}\rangle \tag{A.12}$$

Working out the $e^{(1/2\sum_{i,j}\eta_i^{\dagger(e)}G^\dagger_{ij}\eta_j^{\dagger(e)})}|B^{(e)}\rangle$ part,

$$\begin{aligned}
e^{(1/2\sum_{i,j}\eta_i^{\dagger(e)}G_{ij}\eta_j^{\dagger(e)})}|B^{(e)}\rangle &= \prod_{i,j}\Big[1+\frac{1}{2}G_{ij}\eta_i^{\dagger(e)}\eta_j^{\dagger(e)}+\frac{1}{8}(G_{ij}\eta_i^{\dagger(e)}\eta_j^{\dagger(e)})^2+\dots\Big]|B^{(e)}\rangle \\
&= \prod_{i\neq j}\Big[1+\frac{1}{2}G_{ij}\eta_i^{\dagger(e)}\eta_j^{\dagger(e)}\Big]|B^{(e)}\rangle \\
&= \prod_{i,j>i}\Big[(1+\frac{1}{2}G_{ij}\eta_i^{\dagger(e)}\eta_j^{\dagger(e)})(1+\frac{1}{2}G_{ji}\eta_j^{\dagger(e)}\eta_i^{\dagger(e)})\Big]|B^{(e)}\rangle \\
&= \prod_{i,j>i}\Big[1+G_{ji}\eta_j^{\dagger(e)}\eta_i^{\dagger(e)}\Big]|B^{(e)}\rangle
\end{aligned} \tag{A.13}$$

Here we used the fact that $\eta_l^{\dagger(e)^2}|B^{(e)}\rangle = 0$ and $G_{ji}\eta_j^{\dagger(e)}\eta_i^{\dagger(e)} = G_{ij}\eta_i^{\dagger(e)}\eta_j^{\dagger(e)}$ since $G_{ij} = -G_{ji}$. Similarly, for bra part,

$$\langle B^{(e)}|e^{(1/2\sum_{n,m}\eta_n^{(e)}G^*_{nm}\eta_m^{(e)})} = \langle B^{(e)}|\prod_{m,n>m}\Big[1+G^*_{mn}\eta_n^{\dagger(e)}\eta_m^{\dagger(e)}\Big]. \tag{A.14}$$

Then, $(A.12)$ becomes,

$$\begin{aligned}
\langle B^{(g)}(t)|B^{(e)}(t)\rangle =& \frac{1}{\Upsilon^2}\langle B^{(e)}|\prod_{m,n>m}\Big[1+G^*_{mn}\eta_n^{\dagger(e)}\eta_m^{\dagger(e)}\Big] \\
& e^{iE_0t}\prod_k e^{-i\Lambda_k^{(e)}(\eta_k^{(e)}\eta_k^{(e)}+E_0^{(e)})t}\prod_{i,j>i}\Big[1+G_{ji}\eta_j^{\dagger(e)}\eta_i^{\dagger(e)}\Big]|B^{(e)}\rangle \\
=& \frac{e^{i(E_0-E_0^{(e)})t}}{\Upsilon^2}\langle B^{(e)}|\prod_{m,n>m}\Big[1+G^*_{mn}\eta_n^{\dagger(e)}\eta_m^{\dagger(e)}\Big] \\
& \prod_k e^{-i\Lambda_k^{(e)}(\eta_k^{(e)}\eta_k^{(e)})t}\prod_{i,j>i}\Big[1+G_{ji}\eta_j^{\dagger(e)}\eta_i^{\dagger(e)}\Big]|B^{(e)}\rangle
\end{aligned} \tag{A.15}$$

where we have expressed constant part of excited Hamiltonian as $E_0^{(e)}$. Let's calculate the commutation considering $\eta_k^{(e)}|B^{(e)}\rangle = 0$,

$$\begin{aligned}[\eta_i^\dagger, e^{-it\Lambda_k \eta_k^\dagger \eta_k}] &= e^{-it\Lambda_k}[(\eta_i^\dagger)(1+\eta_k^\dagger\eta_k) - (1+\eta_k^\dagger\eta_k)(\eta_i^\dagger)] \\ &= e^{-it\Lambda_k}(\eta_i^\dagger\eta_k^\dagger\eta_k - \eta_k^\dagger\eta_k\eta_i^\dagger) \\ &= -e^{-it\Lambda_k}\eta_k^\dagger\delta_i k. \end{aligned} \tag{A.16}$$

Using the relation above twice yields,

$$\begin{aligned}&\langle B^{(g)}(t)|B^{(e)}(t)\rangle = \\ &\frac{e^{i(E_0-E_0^{(e)})t}}{\Upsilon^2}\langle B^{(e)}| \prod_{m,n>m}\left[1+G_{mn}^*\eta_n^{\dagger(e)}\eta_m^{\dagger(e)}\right]\prod_{i,j>i}\left[1+e^{-it(\Lambda_i+\Lambda_j)}G_{ji}\eta_j^{\dagger(e)}\eta_i^{\dagger(e)}\right]|B^{(e)}\rangle \\ &= \frac{e^{i(E_0-E_0^{(e)})t}}{\Upsilon^2}\prod_{i,j>i}(1+e^{-it(\Lambda_i+\Lambda_j)}|G_{ij}|^2). \end{aligned} \tag{A.17}$$

So expression $(A.12)$ has been reduced to,

$$|\langle B^{(g)}(t)|B^{(e)}(t)\rangle|^2 = \frac{1}{\Upsilon^4}\prod_{i,j>i}\left[(1+|G_{ij}|^2)^2 - 4(1+|G_{ij}|^2)^2\sin^2\left(\frac{\Lambda_i^{(e)}+\Lambda_j^{(e)}}{2}\right)\right]. \tag{A.18}$$

A.5 Circulant symmetric matrix for uniform coupling regime

Observe that, in (2.32) matrix $(A-B)(A+B)$ is symmetric circulant matrix of the form,

$$C = \begin{pmatrix} c_0 & c_1 & c_2 & \ddots & c_{N-2} & c_{N-1} \\ c_{N-1} & c_0 & c_1 & \ddots & c_{N-3} & c_{N-2} \\ c_{N-2} & c_{N-1} & c_0 & \ddots & c_{N-4} & c_{N-3} \\ \ddots & \ddots & \ddots & \ddots & \ddots & \ddots \\ c_2 & c_3 & c_4 & \ddots & c_0 & c_1 \\ c_1 & c_2 & c_3 & \ddots & c_{N-1} & c_0 \end{pmatrix}, \tag{A.19}$$

has n distinct eigenvectors and eigenvalues,

$$\Phi_k = \begin{pmatrix} 1 \\ \varsigma_k \\ \varsigma_k^2 \\ . \\ . \\ . \\ \varsigma_k^{N-1} \end{pmatrix}, \qquad \Lambda_k^2 = c_0 + c_1\varsigma_k + c_2\varsigma_k^2 + \cdots + c_{N-1}\varsigma_k^{N-1}, \tag{A.20}$$

where $\varsigma_k = e^{ik}$ is the Nth roots solution of 1 ($k = 2\pi m/N, m = 0, \ldots, N-1$). In uniform coupling regime, eigenvalues are,

$$\Lambda_k^2 = (\cos(k) - h)^2 + \gamma^2 \sin^2(k). \tag{A.21}$$

Please note that, If spin couplings are not uniform then the matrix $(A-B)(A+B)$ is no more circulant, meaning $(A.20)$ and $(A.21)$ cannot be used consequently.

A.6 Loschmidt echo for uniform coupling regime

In case of, all chain spins coupled uniformly to each other, $(A.18)$ can be further reduced [35], but instead, it is possible to deduce Loschmidt Echo in more straightforward manner. Start with (2.37),(2.38). Taking Bogoliubov Transformation to connect ground and excited operators [2],

$$\eta^{(g)} = \cos(\alpha_k)\eta_k^{(e)} - i\sin(\alpha_k)\eta_{-k}^{(e)\dagger} \tag{A.22}$$

where,

$$\alpha_k = [\theta_k(\lambda^{(e)}) - \theta_k(\lambda^{(g)})]/2, \tag{A.23}$$

$$\theta_k(\lambda^{(i)}) = \arctan\Big(\frac{\gamma\sin(k)}{\lambda^{(i)} + \cos(k)}\Big). \tag{A.24}$$

[2] What we do is actually same with (2.40).

One can establish connection between, ground and excited states as,

$$|B^{(g)}\rangle = \prod_{k>0}[\cos(\alpha_k) + i\sin(\alpha_k)\eta_k^{(e)\dagger}\eta_{-k}^{(e)\dagger}]|B^{(e)}\rangle. \tag{A.25}$$

Then Loschmidt Echo can be written as,

$$\begin{aligned}
|\langle B^{(g)}(t)|B^{(e)}(t)\rangle|^2 &= |\langle B^{(g)}|e^{-iH^{(e)}t}|B^{(e)}\rangle|^2 \\
&= |\langle B^{(e)}|\prod_{k>0}[\cos(\alpha_k) - i\sin(\alpha_k)\eta_{-k}^{(e)}\eta_k^{(e)}]e^{-iH^{(e)}t} \\
&\times \prod_{k>0}[\cos(\alpha_k) + i\sin(\alpha_k)\eta_k^{(e)\dagger}\eta_{-k}^{(e)\dagger}]|B^{(e)}\rangle|^2 \\
&= |\langle B^{(e)}|\prod_{k>0}[\cos^2(\alpha_k)e^{-iH^{(e)}t} \\
&+ \sin^2(\alpha_k)\eta_{-k}^{(e)}\eta_k^{(e)}e^{-iH^{(e)}t}\eta_k^{(e)\dagger}\eta_{-k}^{(e)\dagger}]|B^{(e)}\rangle|^2
\end{aligned}$$

Now, using the identity, $e^{-iH^{(e)}t}\eta^{(e)\dagger}e^{+iH^{(e)}t} = \eta^{(e)\dagger}e^{-i2\Lambda_k^{(e)}t}$,

$$\begin{aligned}
|\langle B^{(g)}(t)|B^{(e)}(t)\rangle|^2 &= |\langle B^{(e)}|\prod_{k>0}[\cos^2(\alpha_k)e^{-iH^{(e)}t} \\
&+ \sin^2(\alpha_k)\eta_{-k}^{(e)}\eta_k^{(e)}e^{-iH^{(e)}t}\eta_k^{(e)\dagger}e^{+iH^{(e)}t}e^{-iH^{(e)}t}\eta_{-k}^{(e)\dagger}e^{+iH^{(e)}t}e^{-iH^{(e)}t}]|B^{(e)}\rangle|^2 \\
&= |\langle B^{(e)}|\prod_{k>0}[\cos^2(\alpha_k) + e^{-i4\Lambda_k^{(e)}t}\sin^2(\alpha_k)\eta_{-k}^{(e)}\eta_k^{(e)}\eta_k^{(e)\dagger}\eta_{-k}^{(e)\dagger}]|B^{(e)}\rangle|^2 \\
&= |\prod_{k>0}\cos^2(\alpha_k)\sin^2(\alpha_k)e^{-i4\Lambda_k^{(e)}t}|^2 \\
&= \prod_{k>0}^{N/2-1}[1 - \sin^2(2\alpha_k)\sin^2(2\Lambda_k^{(e)}t)].
\end{aligned} \tag{A.26}$$